



Lateglacial and early Holocene evolution of the Tyne Valley in response to climatic shifts and possible paraglacial landscape legacies

Yorke, Lynda; Chiverrell, Richard; Schwenninger, Jean-Luc

Geomorphology

DOI:
[10.1016/j.geomorph.2023.109007](https://doi.org/10.1016/j.geomorph.2023.109007)

Published: 01/02/2024

Peer reviewed version

[Cyswllt i'r cyhoeddiad / Link to publication](#)

Dyfyniad o'r fersiwn a gyhoeddwyd / Citation for published version (APA):
Yorke, L., Chiverrell, R., & Schwenninger, J.-L. (2024). Lateglacial and early Holocene evolution of the Tyne Valley in response to climatic shifts and possible paraglacial landscape legacies. *Geomorphology*, 446, Article 109007. <https://doi.org/10.1016/j.geomorph.2023.109007>

Hawliau Cyffredinol / General rights

Copyright and moral rights for the publications made accessible in the public portal are retained by the authors and/or other copyright owners and it is a condition of accessing publications that users recognise and abide by the legal requirements associated with these rights.

- Users may download and print one copy of any publication from the public portal for the purpose of private study or research.
- You may not further distribute the material or use it for any profit-making activity or commercial gain
- You may freely distribute the URL identifying the publication in the public portal ?

Take down policy

If you believe that this document breaches copyright please contact us providing details, and we will remove access to the work immediately and investigate your claim.

1 Lateglacial and early Holocene evolution of the Tyne Valley in response to climatic
2 shifts and possible paraglacial landscape legacies.

3

4 Yorke, L.¹, Chiverrell, R.C.² and Schwenninger, J-L.³

5 ¹School of Environmental & Natural Sciences, Bangor University, Thoday Building, Bangor, LL57
6 2UW.

7 ²Department of Geography and Planning, School of Environmental Sciences, University of
8 Liverpool, Roxby Building, Liverpool, L69 7ZT.

9 ³Research Laboratory for Archaeology and the History of Art, School of Archaeology, University of
10 Oxford, Dyson Perrins Building, Oxford, OX1 3QY.

11

12 **Abstract**

13 This paper presents new sedimentological, geomorphological, and optically stimulated
14 luminescence (OSL) geochronological evidence for fluvial evolution of the mid- to lower River
15 Tyne through the Lateglacial to late Holocene. These data reveal a series of fluvial terraces
16 produced by cycles of aggradation and incision, conditioned by glacial inheritance and driven by
17 changing sediment availability and hydrological regime. The distribution and stratigraphy (where
18 available) of nine river terrace and their associated sediments have been recorded. At two key
19 sites the sediments have been dated using OSL measurements to constrain the fluvial
20 geomorphology. Significant entrenchment of the fluvial system, followed by aggradation formed
21 the earliest fluvial terrace (T1), which encompasses environments spanning the transition from
22 deglaciation into Greenland Interstadial 1 (GI-1). Incision below T1 began towards the end of GI-
23 1, with three terraces (T2 – T4) between the abandonment of T1 and the early Holocene (15.0 –
24 9.2 ka). Climatic shifts, limited vegetation cover/soil development, and peri-/paraglacial landscape
25 instability conditioned the development of the early postglacial fluvial landsystem. Three further
26 terraces (T5 – T7) developed during the mid- to Late Holocene (6.6 – 3.1 ka), and comprise most
27 of the valley floor. Climatic instability, glacial inheritance, and widespread anthropogenic

28 disturbances are reflected in greater hillslope-channel coupling during this period. The extent of
29 later Holocene terraces (T8 – T9) is limited as the river became isolated from flanking hillslopes
30 entrenched between existing river terraces. Fluvial landscape evolution in formerly glaciated
31 catchments is strongly conditioned by the cold stage legacy that introduced excess sediment and
32 landscape instability into the catchment. Subsequent catchment-wide responses are variable and
33 non-linear, with valley floors operating in a series of reach-wide responses. There is a need for
34 greater chronological control to constrain the Lateglacial and Holocene evolution in the Tyne
35 catchment, but also to further our understanding of region-wide responses to external drivers and
36 local dynamics.

37

38 **Abbreviations:** BIIS, British-Irish Ice Stream; BSW, Bog Surface Wetness; CAM, Central Age
39 Model; DEM, Digital Elevation Model; GI, Greenland Interstadial; GI, Greenland Stadial; LGM,
40 Last Glacial Maximum; LiDAR, Light Detection and Ranging; MAM, Minimum Age Model; MIS,
41 Marine Isotope Stage; NSL, North Sea Lobe; OD, Ordnance Datum; OSL, Optically Stimulated
42 Luminescence; SAR, Single aliquot regeneration; TGIS, Tyne Gap Ice Stream; YDS, Younger
43 Dryas Stadial.

44

45 **Keywords:** Lateglacial; Fluvial development; Glacial legacy; Climatic shifts; Tyne valley

46

47 Correspondence to: Lynda Yorke email: l.yorke@bangor.ac.uk

48 1. Introduction

49 River terraces and their deposits are important archives of terrestrial environmental change and
50 catchment sediment dynamics, as such they can reveal the response of fluvial systems to
51 external forcing (e.g. climate and extreme events; base-level change; vegetation and land cover;
52 and, anthropogenic activities) and internal fluvial dynamics. The degree of fluvial response to
53 driving forces is often linked to landscape and river sensitivity (cf. Brunnsden and Thornes, 1979;
54 Fryirs, 2017), with sediment availability a major driver of geomorphic change. Changes in
55 sediment flux can result in channel incision/aggradation, floodplain aggradation, and lateral

56 channel migration. Additionally, local fluvial dynamics and discontinuities between and within
57 reaches can mute or amplify the response to external drivers (Chiverrell et al., 2010; Philips,
58 2010). However, compared to other European river systems, the timescales and responses of
59 British rivers, within the limits of the British-Irish Ice Sheet (BIIS; MIS 2), during the Lateglacial
60 and early Holocene are poorly constrained, especially in contrast to lowland systems that lay
61 beyond the BIIS (Collins et al., 2006; Gao et al., 2007; Lewin and Gibbard, 2010; Brown et al.,
62 2013). Accurately dated fluvial landform sequences in the uplands and piedmont zones of
63 systems within the MIS 2 ice sheet limit are rare in the UK for this period (Macklin and Lewin,
64 1993; Macklin et al., 2014), making it difficult to explore potential relationships between fluvial
65 dynamics and forcing factors. Some important exceptions are available from northern Britain,
66 however. There are dated sequences from both the eastern and western Pennine rivers such as
67 the Wharfe (Howard et al., 2000a), Swale (Taylor et al., 2000) and Ure (Howard et al., 2000b;
68 Bridgland et al., 2011), Hodder and Ribble (Chiverrell et al., 2009a; Foster et al., 2009) and, in
69 Scotland the Kelvin, Feshie and Spey (Tipping et al., 2008; Ballantyne, 2019; Werritty, 2021).

70

71 Conceptual models of responses of fluvial systems through glacial-interglacial cycles in Northwest
72 Europe indicate channel instability and channel pattern change, followed by aggradation and
73 stability (Vandenberghe, 2008; Kaiser et al., 2012). In the UK, transitions from cold-to-warm have
74 typically been associated with channel incision and erosion, coupled with shifts from a braided
75 river system to a meandering river system (e.g. Maizels, 1982; Bridgland, 2000; Chiverrell et al.,
76 2009a; Macklin et al., 2013). Short-lived climatic oscillations (warm-to-cold), such as the Bølling-
77 Allerød to Younger Dryas, have been recorded as catchment instability and aggradational
78 episodes in lowland systems (Hill et al., 2008; Howard et al., 2011). The transition from the BIIS
79 (MIS 2) glacial land-system to post-glacial fluvial system encompassed the climatic changes in
80 the late glacial (GI-1 and GS-1) and the early Holocene climate events (Mayewski et al., 2004;
81 Lowe et al., 2008; Lang et al., 2010; Shakun and Carlson, 2010; Thornalley et al., 2009;
82 Rasmussen et al., 2014). The transition into the early Holocene in northern England was also
83 accompanied by base-level changes, linked to lower than present sea levels (Bradley et al., 2011;

84 Shennan et al., 2012) and glacio-isostatic uplift (Bridgland et al., 2010; Bridgland and Westaway,
85 2014). The fluvial system changed from glacial to nival-fed (snowmelt) discharge regimes to
86 temperate systems, and was marked by reductions in sediment availability reflecting both
87 exhaustion (cf. Church and Ryder, 1972) and landscape stabilisation with vegetation and soil
88 cover. Thus, a paraglacial landsystem conceptual model (cf. Ballantyne, 2005; Harrison et al.,
89 2010) describes the post-glacial development of upland formerly glaciated catchments and
90 describes the evolution of sediment regimes inside the last glacial maximum (LGM) limits. In this
91 model the postglacial hillslope processes and fluvial systems of Britain are out of phase with
92 major climatic shifts, thus the redistribution/availability of the sediment is important and may act
93 as a lead or lag in fluvial development.

94

95 Northern England lies within the limits of MIS 2 ice and many river valleys, including the Tyne, are
96 infilled with glacial, soliflucted, colluvial and fluvial deposits. Previous workers have investigated
97 reaches in the Tyne basin during the mid and late Holocene period (e.g. Passmore and Macklin,
98 1994; Rumsby and Macklin, 1996), but these studies did not concentrate on the Lateglacial–
99 Holocene transition. Here, we present evidence for fluvial development for a 22 km stretch of the
100 piedmont middle Tyne valley. Our aims are: (i) to present the alluvial landform record; (ii) to
101 identify the sequence of valley-floor development; (iii) to interpret the depositional environment
102 from the sedimentary record; (iv) to establish a chronological framework using optically stimulated
103 luminescence dating (OSL); (v) to explore the response of the fluvial system to climate change
104 and other conditioning factors.

105 **2. Study area**

106 **2.1. The Tyne Basin**

107 The Tyne basin lies in the northeast of England (Fig. 1) and comprises a catchment area of 2,936
108 km². The Tyne basin (maximum elevation 893 m) comprises two main tributaries; the North Tyne
109 rises on the Cheviot Hills near the Scottish border and the South Tyne forms on the North
110 Pennines near the Cumbrian border. These tributaries combine near Hexham (Fig. 1) to form the
111 River Tyne. The river Tyne is 118 km in length, and reaches the north sea at Tynemouth.

112 Geologically, the basin is underlain by Carboniferous limestone, sandstone, siltstone and
113 mudstone, along with Silurian greywackes and Devonian sandstones. Andesite outcrops in the
114 Cheviot Hills, whilst Dolerite is found along the south Tyne. Structurally, the Alston block and
115 Northumberland fault-trough bound the catchment (Scrutton, 1995; Johnson, 1997). Investigation
116 focused on the mid-Tyne valley (w-e flowing section), extending as far upstream as the Allen
117 confluence (South Tyne) and as far downstream as Broomhaugh (Tyne) (Fig. 1). The Tyne valley
118 comprises wide valley floors (or basins), with occasional narrow sections (or gorges), and the
119 present day river can be described as a wandering/meandering gravel-bed river.

120

121 During the last glaciation northern England and the Tyne valley were overridden by British-Irish
122 Ice Sheet (BIIS) (Hughes et al., 2016). Regionally, the ice was around 0.8 km thick at the LGM. A
123 west-east flowing ice stream (Tyne Gap Ice Stream; TGIS) extended along the Tyne valley
124 (Smith, 1994; Mills and Holliday, 1998; Livingstone et al., 2012, 2015) and an ice lobe extended
125 north-south down the North Sea coast (North Sea Lobe; NSL). Constrained by Bayesian
126 statistical analysis of radiocarbon and cosmogenic ages, retreat of the TGIS had begun by 18.5–
127 18.3 ka (Livingstone et al., 2012, 2015; Evans et al., 2021; Clark et al., 2022), creating
128 accommodation space in the mid and lower Tyne valley as it decoupled from the NSL impounding
129 waters in the Tyne lowlands. In the Tyne valley an extensive pro-glacial drainage system
130 developed feeding water and sediments towards a large ice-dammed lake (Glacial Lake Wear)
131 (Smith, 1994; Davies et al., 2009; Yorke et al., 2012; Teasdale, 2013). The NSL had retreated
132 completely from the east coast by 17–16.5 ka (Roberts et al., 2018; Evans et al., 2021), with ice
133 retreating to the upland dispersal centres (Lake District) by 17 ka (Davies et al., 2019). Following
134 deglaciation, regional sea levels were low, lying at -30 m Ordnance Datum (OD) at 12 ka BP
135 (Bradley et al., 2011). Buried peats within estuarine sediments found in the lower Tyne constrain
136 early Holocene marine inundation to 8.5 ka cal. BP (Horton et al., 1999a,b). Glacio-isostatic uplift
137 across Northumberland has declined since deglaciation, with a present-day uplift rate of 0.2–0.8
138 mm a⁻¹ south to north respectively (Bradley et al., 2011; Shennan et al., 2012; Bradley et al.,

139 2023). Base-level change for regional river systems, driven by both eustatic and glacio-isostatic
140 factors, may have influenced fluvial dynamics during the Lateglacial and early Holocene period.
141

142 This study focuses on three reaches. Zone I is a lowland reach set within ice-disintegration
143 topography, where narrow valley floor fluvial terraces are preserved on inner meander banks
144 between the Allen confluence and a knick-point gorge (Newbrough) upstream of Fourstones.
145 Zone II is a gently meandering reach that straddles the confluence of North and South Tyne, with
146 terraces preserved on both sides of the valley floor flanked by subglacial features between
147 Fourstones and Acomb. Zone III is a major alluvial basin (Corbridge) between Hexham and
148 Broomhaugh (Fig. 1), with extensive valley floor fluvial terraces present set below extensive
149 glacial outwash deposits.

150 **3. Materials and methods**

151 3.1. Geomorphological mapping

152 Mapping of the valley floor features drew on interpretation of Light Detection and Ranging
153 (LiDAR) digital elevation model (DEM), supplied by the Environment Agency's Geomatics Group.
154 The LiDAR DEM had a spatial resolution of 1 m², with a vertical accuracy of ~0.15 m. Mapping
155 was undertaken using the interpretative tools within ArcGIS. Extensive flat areas and linear
156 depressions reflect and were digitised as river terrace fragments and palaeochannels
157 respectively. Identification was possible through manipulation of the DEM to produce hill-shaded
158 surfaces, narrow elevation range shaded DEMs and interval contours. Field mapped data were
159 used to 'ground-validate' the terrace fragments and palaeochannels interpreted from the LiDAR
160 DEM at scales of 1: 10,000.

161 3.2. Sedimentological investigations

162 The sediments underlying the mapped terraces were recorded from river-bank exposures and
163 using closely spaced sediment profiles interpreted from the British Geological Survey (BGS)
164 online database of borehole logs. Sediment analysis followed a lithofacies approach (Miall, 1988)
165 and sediments were recorded on the basis of grain size, bed contact and bedding, sorting and

166 texture, sedimentary structures, colour, and sediment body geometry (Jones et al., 1999). Clast
167 form and provenance was established by clast (>0.05 m) lithological analysis (Bridgland, 1986).
168 Established fluvial form-process models (Miall, 1996) underpin interpretations of lithofacies and
169 helped interpretation of the generalised vertical succession.

170 3.3. Optically Stimulated Luminescence dating

171 In the absence of *in situ* organic material for radiocarbon dating, to develop a chronology for the
172 terrace sequence we used Optically Stimulated Luminescence (OSL) dating to target sands within
173 terraces 1, 4, 5 and 7. Suitable lithofacies that had the greatest potential to have been exposed to
174 light prior to deposition (cf. Thrasher et al., 2009) were targeted for OSL dating, e.g. overbank and
175 bar-top sands. Samples were collected (in daylight) by hammering opaque plastic tubes (300 x 50
176 mm) into cleaned faces. Bulk materials collected within 30 cm of the OSL sample provide
177 materials for measurement of moisture content and γ dose rate in the laboratory. Sand-sized
178 quartz (180-255 μ m or 90-125 μ m) mineral grains were extracted from the sediment samples using
179 standard preparation techniques. These included wet sieving, removal of organic matter using
180 H₂O₂ (10%), HCl (10%) treatment to remove carbonates, HF (48%) treatment for 60 minutes
181 followed by an additional etching in H₂SiF₆ acid for two weeks to dissolve remaining feldspathic
182 components as well as heavy mineral separation using sodium polytungstate (2.63g cm⁻³). All the
183 samples were measured as medium sized (4mm diameter) multigrain aliquots mounted on
184 aluminium discs inside an automated Risø TL/DA15 luminescence reader (Bøtter-Jensen 1997,
185 2000) using a SAR post-IR blue OSL measurement protocol (Murray and Wintle, 2000; Banerjee
186 et al., 2001; Wintle and Murray, 2006). Due to the fluvial nature of the sediments and in order to
187 avoid overestimating the true depositional age of the sediments as a result of incomplete
188 bleaching of the OSL signal (Murray et al. 1995, Wallinga 2002), the D_e estimates were calculated
189 using a Minimum Age Model (Galbraith et al. 1999) within the 'R' statistical programming
190 language (Kreutzer et al. 2012). Dose rate calculations are based on the concentrations of
191 radioactive elements (potassium, thorium, uranium and rubidium) within the sediment. These
192 were derived from elemental analysis performed by Actlabs (Canada) using induced coupled
193 plasma mass spectroscopy / atomic emission spectroscopy (ICP-MS/AES) and a fusion sample

194 preparation technique. The final OSL age estimates include an additional 2% systematic error to
195 account for uncertainties in source calibration. Dose rate and age calculations were obtained
196 using DRAC version 1.2 developed by Durcan et al. (2015). These are based on Aitken (1985)
197 and incorporated updated grain size attenuation factors of Brennan et al. (1991) and Guerin et al.
198 (2012), etch depth attenuation factors of Bell (1979), dose rate conversion factors of Guerin et al.
199 (2011) and an absorption coefficient for the water content. The contribution of cosmic radiation to
200 the total dose rate was calculated as a function of latitude, altitude, burial depth and average
201 over-burden density based on data by Prescott and Hutton (1994). The OSL age estimates
202 (presented as ka: Table 1) include an additional 2% systematic error to account for uncertainties
203 in source calibration.

204 **4. Results**

205 4.1. Fluvial geomorphology

206 Across the three zones (Fig. 1) of the mid-Tyne valley, the geomorphology and longitudinal
207 height-range relationships reveal nine fluvial terraces that lie between 20 and 2 m above present
208 river level (T1 – T9; highest to lowest) and the modern floodplain (Fig. 2 and Fig. 3). T1, broadly
209 20 m above the modern river, comprises fragmented surfaces that lie along the valley margins of
210 the South Tyne system. However, within zone III the surfaces are laterally extensive (Fig. 2c) and
211 show some continuity with extensive glaci-fluvial/-lacustrine deposits (Yorke, 2008) in terms of
212 extent, however, they are inset ~10m below the glaciogenic surfaces. T2 lies at 15 m above
213 modern river level and is restricted to isolated fragments located towards the outer margins of the
214 valley, with greater lateral extent in the South Tyne upstream of Newbrough Gorge (zone I). It is
215 present most extensively around the confluence of the North and South Tyne (zone II), and forms
216 a component of an alluvial fan at Dilston (Fig. 2c). T3, 14 m above modern river level, is laterally
217 extensive in zone I along the South Tyne above Newbrough Gorge (Fig. 2a), and restricted to
218 isolated fragments in zones II-III downstream of Newbrough Gorge, and in the area around the
219 town of Corbridge, hereafter referred to as the Corbridge Basin (Fig. 2b). This upper group of
220 terraces lack any surface palaeochannel topography and are altitudinally separated by 8 m from

221 the lower terraces T5 – T9. Their elevated, fragmentary and valley margin nature reflects that
222 they are terrace remnants preserved in less active sectors of the former floodplain, with removal
223 from the main channel belt during subsequent fluvial erosion and basal incision that generated
224 terraces T4 – T9.

225

226 T4, at 9 m above current river level, occurs throughout zones I to III, but is most extensive in zone
227 III, the Corbridge Basin. The terrace long profile shows a reduction in gradient downstream from
228 0.05 to 0.01, and lies closer in elevation to the present river downstream (9 to 6 m above river
229 level). Several sinuous (sinuosity index 1.3) palaeochannels are visible on T4 (zone III), indicating
230 a meandering system and suggesting some lateral stability of channel systems. T5 lies 6 m above
231 the base of the modern river and has limited presence throughout the study area. T5 grades into
232 the Newbrough Gorge. Numerous surficial palaeochannels are evident on this terrace, and their
233 planform sinuosity is almost straight (sinuosity index <1.05). The channels show evidence of
234 progressive lateral change through avulsion and chute cutoffs. T6 lies 5 m above the bed of the
235 present river and is present in all zones, I – III. T6 extensively occupies the meander bend within
236 zone III. Surficial palaeochannels are ubiquitous on this terrace, and whilst sinuosity is straight to
237 low (sinuosity index <1.05–1.03), in zones II – III channel planforms indicate bar progradation and
238 downstream translation of the meander bend. Migration within these palaeochannels is similar to
239 the development of the present-day meanders. T7 is only present in zones I – II, lies 4 m above
240 the modern river and is sculpted with extensive palaeochannels. Their morphology reflects a low-
241 sinuosity (sinuosity index 1.06–1.30) planform, with lateral valley-floor channel migration through
242 avulsion and chute cut-offs.

243

244 T8 and T9 are the least extensive terraces recorded in the main Tyne valley. T8 lies 3 m above
245 the base of the modern river, and is present in zone II immediately upstream and downstream of
246 the Tyne confluence. T9 lies 2 m above the present river, occurs as discrete deposits along the
247 inner banks of the meanders in zone I (Allen Fan), and in zone III associated with the Dilston Fan
248 (zone III). Both T8 and T9 reflect the most recent depositional activity of the river.

249

250 The South Tyne valley-floor (zones I–II), through to the confluence, is dominated by T6 and T7,
251 bounded by the higher T1 to T4. T6 and T7 form a significant sediment depocenter (*sensu*
252 Chiverrell et al., 2010) in the South Tyne accounting for >90% of the valley floor. Zone III
253 continues to be dominated by T6, accounting for >80% of the valley floor and represents another
254 significant depocentre. Zone II forms a division, separating the higher T5 of the South Tyne
255 system from the lower T6 and T7 of the River Tyne. The narrow Newbrough Gorge, South Tyne,
256 with its lack of valley floor provides a natural break in the terrace sequence.

257

258 Alluvial fans have formed at the mouths of a number of small tributaries but two significant fans
259 are found at confluences of the River Allen (zone I) and Devil's Water (Dilston Fan, zone III). The
260 Allen Fan terrace sequence comprises T6 and T7 and is coherent with the terraces in the South
261 Tyne, and suggests a younger development of this fan. The Dilston Fan terrace sequence
262 comprises an older sequence of terraces, with T1 to T5 present, with T5 grading into the valley-
263 floor sequence. The Dilston Fan represents a long history of formation that corresponds with the
264 Lateglacial and Holocene fluvial development of the Tyne fluvial terraces.

265 4.2. Sediments and geochronology

266 Exposure of the fluvial succession adjacent to the modern channel is restricted to cut-bank
267 exposures at Fourstones (Zone II) and Farnley Haugh (Zone III) which reveal detail on the
268 stratigraphy of T1, 4, 5 and 7. Borehole logs (from the BGS archive) provided additional sub-
269 surface stratigraphy for T1, 6 and 7.

270

271 4.2.1. The A69 (Zone II) and A68 (Zone III) borehole series

272 Borehole logs from the construction of the A69 (near Hexham) and A68 roads (near Broomhaugh)
273 show the sediment stratigraphy (Fig. 4a,b) extending to bedrock revealing a significant infill of
274 basal sediments in the Tyne valley (Fig. 5a,b). The profile indicates incision into bedrock to ~10 m
275 OD and the undulations in the bedrock surface reflect a former channel position. This channel is
276 offset from the current day river, and has a channel base falling from 0 m OD below zone II to -30

277 m OD near the estuary (Cumming, 1971, 1977). The incision of the bedrock valley probably
278 reflects some glacial deepening by ice draining the Tyne Gap and North Tyne Valley, and/or
279 earlier fluvial incision under lower eustatic sea levels (Cox, 1983; Mills and Holliday, 1998). The
280 channel forms a palaeovalley to the north of the present-day river. The valley sediment fill
281 comprises basal over-consolidated diamicts ~5 m thick. Moving downstream the palaeovalley
282 (Fig. 6) the glacial diamict thickens towards the valley centre (~15 m thick), and is overlain by
283 pro-glacial sands and sandy gravels of varying from 10 to >15 m in thickness (Fig. 5, 6). This
284 sequence records the presence of ice in the region, and the subsequent ice retreat with the
285 development of the pro-glacial drainage system (Yorke et al., 2012; Livingstone et al., 2012). The
286 basal sediments represent >20 m of aggradation and were likely deposited between 30 and 15 ka
287 BP (Livingstone et al., 2015). The upper bounding surface of these glacigenic sediments forms a
288 base to the overlying post-glacial fluvial succession.

289

290 The A68 borehole series crosses the valley-floor, revealing the composition of T1 and T4 (Fig. 4b,
291 5b). T4 shows incision to a diamict surface, and subsequent aggradation of ~6 m of sandy
292 gravels, overlain by ~10 m of silty, gravelly sands and capped by 1-2 m of silty sands. The
293 sedimentary sequence and palaeochannels visible on the surface of T4 suggest a meandering
294 fluvial system. The A69 borehole series crosses both T6 and T7 (Fig. 4a, 5a) recording for T6 a
295 basal post-glacial unit of ~7 m thick sandy gravels, with occasional silty sands. Towards the outer
296 margins of the valley within T6 there are three discrete units cut into the sandy gravels. These
297 units comprise a channel fill of <2 m laminated peat and peaty silt, and the whole sequence is
298 buried by 4 m of laminated silts. Well-developed meanders and scroll-bar forms on T6
299 downstream of Newbrough Gorge (zone II) identify lateral migration of the channel reflecting
300 increased sediment mobility and stream power. Meandering and migration of scroll-bars has led
301 to development of 'peaty' back-channel swamp environments with channel migration (Hooke,
302 2003, 2004; van de Lageweg et al., 2014). For T7, ~7 m of sandy gravels overlie the diamict,
303 capped by ~1 m of laminated silty sands. Both the T6 and T7 sequences suggest a transition
304 from a high-energy channel to a low-energy system. The sandy gravels reflect bedload deposition

305 within the main channel, with the silty sands indicative of overbank deposition. The silty sands of
306 T7 exposed at Fourstones and were targeted for OSL dating (X2733) to constrain the meandering
307 and scroll-bar progradation associated with T6 – T7.

308

309 4.2.2. Exposures at Farnley Haughs

310 Near Farnley Haughs (zone III) a 20 m long erosion scar (Fig. 6a) exposes the sediments
311 comprising T1. Thinly laminated, very fine basal sands are interpreted as subaqueous glacio-
312 fluvial sediments (Yorke et al., 2012). High elevation valley-side glacial outwash terraces reflect a
313 proglacial drainage system entering Glacial Lake Wear, dammed by the NSL to the east (Smith,
314 1994; Yorke et al., 2012; Davies et al., 2019). This unit is overlain unconformably by ~4 m of
315 fluvial sediments comprising rounded cobbles, forming a concave channel lag deposit at the base
316 of the post-glacial sequence. Above the channel lag are rounded, clast- to matrix-supported
317 gravels (predominantly Carboniferous sandstones and greywacke, and igneous clasts inc. Shap
318 granite originating from the Lake District), which reflect vertical accretion as longitudinal bars, with
319 initial aggradation in low water from tractional processes and small-scale structures
320 superimposed on the larger bedforms during waning flow (Miall, 1996; Bridge, 2009; Rice et al.,
321 2009). The longitudinal bars are intercalated with coarse sandy gravel, pebbly sands and silty
322 sands, which indicates fluctuating flows (Smith et al., 2009; Rice and Church, 2010) (Fig. 6b).
323 Laminated fine sands (2 m thickness), indicative of overbank deposition, cap the sequence and
324 are typical of floodplains adjacent to shallow, wandering gravel-bed river (Miall, 1996). The upper
325 sands were sampled for OSL dating (X2734; Fig. 6b) to constrain late-stage aggradation of T1
326 and provide a younger than constraint on the incision to T2.

327

328 4.2.3. Exposures at Fourstones

329 T4 and T5 were examined through a cut-bank section that exposes 0.5 km of sediments, opposite
330 the town of Fourstones (zone II) (Fig. 7a). For T4, the section reveals a basal till (which forms the
331 stream bed), overlain by ~4 m of well-rounded, weakly horizontal-stratified to structureless
332 cobble- and boulder-rich gravels (a-axis up to 120 cm) that are indurated with iron-manganese

333 coatings and imbrication is well developed. Clasts within T4 are predominantly volcanic and
334 igneous in origin (81%), with fewer Carboniferous sandstones, limestones and mudstones (19%).
335 This matches the clast lithologies recorded within the till (predominantly Lake District volcanic and
336 igneous clasts – dolerite, quartzite and granite, with subordinate amounts of Carboniferous
337 sedimentary clasts), indicating that the river reworked earlier sequences. A chute channel
338 truncates the gravel at the downstream end of T4, and is infilled with cross-stratified to massive
339 cobble- and pebble-sized sandy gravel, indicative of high relief bar edges, overlain by laminated
340 sands. Chronological control for T4 was obtained from the laminated sands (X2730) (Fig. 7b).
341 The stratified gravels represent bedload, with sorting, imbrication and iron-coatings all indicate
342 transport and deposition in shallow water/fluctuating water levels. The presence of large boulders,
343 structureless gravels, chute channel and bar deposits in the upper 2 m suggests higher-
344 magnitude flows (Desloges and Church 1987; Smith, 1990; Brierley and Hickin, 1991). The
345 sequence is interpreted as a wandering gravel-bed system (Miall, 1996), with periods of lateral
346 channel instability during extreme flow events (Wooldridge and Hicken, 2005).

347

348 For T5, the sequence displayed extensive exposure of the basal lodgement till (~2 m). The fluvial
349 sediments of T5 appear to reflect a large remnant palaeochannel, channel bed deposits and
350 occasional infilled chute channels. The palaeochannel sediments form the boundary between T4
351 and 5, comprising ~4 m of laminated to massive sands, overlain by a silty sandy clay, with
352 intercalated sandy gravel layers (Fig. 7b). The sands were sampled for OSL dating (X2731;
353 X2732). The basal sands probably formed under upper flow regime conditions (Smith, 1990;
354 Tucker, 2011), with the overlying sandy clays and intercalated gravels suggesting slower flows
355 with occasional fluctuations in stream competence (Miall, 1996; Bridge, 2009). The sands grade
356 (downstream) into a sequence of horizontally bedded gravel, with intercalated sands (~6 m thick),
357 capped by laminated sands (~1 m thick). The gravels comprised 47% volcanic and igneous
358 clasts, with 52% Carboniferous sandstones and mudstones, and sub-ordinate amounts of coal.
359 The gravel geometry suggests development of longitudinal bars in shallow water, (Whiting et al.,
360 1988; Miall, 1996). Periods of lateral instability and high-energy flows are indicated by the multi-

361 storey layers of inversely graded clast- to matrix-supported cobble- and pebble-sized gravel, and
362 thinly laminated sands, cut into the sands. Within the gravels, chute channels are infilled with
363 laminated silty clays and suggest channel migration and abandonment, with deposition under
364 slack water conditions (Smith, 1990; Miall, 1996). The silty clays provided an opportunity for OSL
365 dating T5 (X2832). The sequence represents the main channel belt, with deposition towards the
366 outer margins of the valley floor, and is typical of a wandering gravel bed system (Miall, 1996).

367

368 4.3. Geochronology and fluvial sequence

369 The new geochronological control obtained for T1, 4, 5 and 7 of the Tyne sequence, alongside
370 two existing ^{14}C ages of 5900 ± 70 cal. BP (BETA-37060) for T5 (tree trunk in basal gravels) at
371 Farnley Haughs (Passmore and Macklin, 1994) and 3030 ± 60 cal. BP (BETA-45549) for T7 (wood
372 fragments within a basal channel incised into till) at Lambley (Fig. 1, ~13km upstream of the Allen
373 confluence; Passmore and Macklin, 2000) provide a basis for exploring the landform sequence.
374 We discounted Passmore and Macklin's (1994) OSL age of 2.45 ± 3.5 ka obtained from T5
375 (upper sequence channel fill sandy silts) at Farnley Haughs on the basis that it was obtained 30
376 years ago. Significant improvements in techniques and instrumentation in the last 20 years have
377 occurred and it was not until post-1999 that OSL dating protocols became more reliable (Wintle,
378 2008; Mahan et al., 2022). We have employed an approach, using OxCal (Bronk Ramsey, 2001),
379 that facilitates statistical testing of these theoretical models of the likely relative order of events in
380 the Tyne geomorphology (Chiverrell et al., 2009b). Bayesian assessment using OxCal of these
381 relative order models (Bronk Ramsey, 2008) helps with identification (Fig. 8) of anomalous ages
382 that are nonconformable and/or out of sequence (Buck et al., 1996; Chiverrell et al., 2009b). The
383 objective with the dating was to constrain the timing of switches between river terrace levels, but
384 these are rarely dated directly, typically sitting as erosion episodes between landforms and
385 derived ages. The Bayesian models were coded in OxCal v4.4.4 Bronk Ramsey (2021) and using
386 the INTCAL20 atmospheric data from Reimer et al. (2020) as a Sequence model. The Prior
387 models in Bayesian nomenclature are structured as a series of Phases, which are unordered
388 groups of events/parameters that contain age information e.g. the differing individual river

389 terraces. Boundaries, in the OxCal nomenclature, use the relationships between dated individual
390 samples or Phases to generate estimated age probability ranges for undated events (e.g., T1 to
391 T4 Boundary in Fig. 7). The Tyne model (Fig. 8) has an overall agreement index of 90%
392 exceeding the >60% threshold advocated by Bronk Ramsey (2009). This level of agreement was
393 achieved by handling three OSL ages as 100% outliers as detailed below.

394

395 OSL ages obtained from overbank sands at Fourstones (zone II) and Farnley (zone III) (Table 1)
396 alongside the published ^{14}C age (tree trunk within basal gravels of our T4; Passmore and Macklin,
397 1994) help to establish an outline geochronological framework for the Tyne terraces. The
398 uppermost alluvial sediments of T1 (Farnley) provided an OSL age (X2734) of 12.9 ± 1 ka (Fig.
399 9a). T2 and T3 remained undated, but the top of the T4 (Fourstones) sequence yielded an OSL
400 age (X2730) of 10.7 ± 1.1 ka (Fig. 9b). Samples from T5 (X2731; X2732; X2832) returned OSL
401 ages suggestive of poor resetting of the OSL signal and were regarded on that basis as too old.
402 The uppermost sediments of T7 (Fourstones) yielded an OSL age (X2733) of 3.2 ± 0.5 ka (Fig.
403 9c). Though not dated here historic map data suggest that T8 and T9 relate to the last 300 years.
404 The OSL ages obtained suggest the major terraces developed during the Lateglacial to mid-
405 Holocene period. The Bayesian modelling has calculated modelled age probability distributions
406 for the evolution of the Tyne terraces, constraining the T1 / Deglacial transition to 16.0 ± 2.1 ka,
407 the progression from T1 to T4 to 11.9 ± 2.7 ka, T4 to T5 to 8.7 ± 2.3 ka, and T5 to T7 4.0 ± 1.8 ka.
408

409 **5. Discussion**

410 **5.1. Late MIS 2 to GI-1**

411 In northern Britain, landscape development with deglaciation responded to the progressive retreat
412 of the TGIS, with regional ice retreat models indicating that the Tyne valley deglaciated before
413 16.4–15.7 ka during a regional collapse of ice dispersal centres. As changes to ice drainage
414 routeways developed with deglaciation more local topographical control of ice became dominant
415 (Hughes et al., 2014; Livingstone et al., 2015; Davies et al., 2019). An extensive proglacial

416 drainage network developed in the Tyne draining towards Glacial Lake Wear (Yorke et al., 2012),
417 which formed between 17.0 and 16.5 ka as the NSL extended across the lowlands impounding
418 glacial meltwaters (Smith, 1994; Bateman et al., 2011; Davies et al., 2019). Ice marginal
419 glaciofluvial and glaciolacustrine sediments aggraded against the retreating and decaying Tyne
420 Gap Ice Stream, forming a series of valley side outwash terraces (Peel, 1941; Mills and Halliday,
421 1998; Yorke, 2008; Livingston et al., 2015). The highest outwash deposits lie at between 30 and
422 40 m above the base of the present river, and likely aggraded during the period 16.0 ± 2.1 ka.

423

424 The earliest of the Tyne fluvial terraces (T1) are inset 10 m below the lowest outwash surface. An
425 OSL age (X2734) obtained from the overbank sands of T1 dates indicates fluvial aggradation up
426 to 12.9 ± 1 ka and implies the river was active during the Interstadial (GI-1). T1 comprises coarse
427 gravels, intercalated with sandy layers and capped by fine silty sands, typical of channel and bar
428 features and material deposited from overbank flows. The fluvial system is considered to be
429 meandering, with episodic flooding events and intermittent fluvial-lacustrine conditions (Gibbard
430 and Lewin, 2002), possibly developing during the earliest phase (GI-1e/d) before the landscape
431 stabilised and vegetation cover (i.e. *Betula*, *Juniperus*) became established (Innes et al., 2021).
432 The upper part of the unit represents repeated overbank deposition and suggests the channel
433 had already begun to incise or laterally migrate during the latter stages of the Interstadial, with
434 this area of active channel replaced by floodplain aggradation (Vandenberghe, 2015).

435

436 5.2. GS-1 to early Holocene

437 Between the onset of GS-1 and the early Holocene, the OSL ages obtained from T1 and T4 (12.9
438 ± 1 ka and 10.7 ± 1 ka) imply cycles of fluvial incision and aggradation characterised the
439 transitional phase of the Lateglacial period. The event boundary creates a timeframe of 13.3 to
440 10.4 ka for the development of this upper group of terraces. Cooling at the transition between GI-
441 1a and GS-1 signified a return to cold stage conditions (Bakke et al., 2009). The partially wooded
442 conditions established during GI-1 were impacted by the periglacial conditions, with open

443 woodland and shrub-heath replaced by sedge-tundra open herbaceous vegetation (Innes, 1999;
444 Innes et al., 2021).

445

446 The absence of accessible sediments prevents an interpretation of T2 and T3, however, T2
447 represents incision and aggradation after 12.9 ka. If we assume they are cut and fill rather than
448 erosional terraces (Lewin and Macklin, 2003 suggest renewed aggradation during GI-1) then their
449 development can be linked to hydrological and landscape change during GI-1. We infer that
450 geomorphic activity was strongly conditioned by periglacial slope processes and paraglacial
451 adjustment during GI-1 (Chiverrell et al., 2007; Passmore and Waddington, 2009; Ballantyne,
452 2019; Harrison et al., 2021), driven by nival flow and spring flood runoff, creating a sediment-
453 dominated fluvial system. T4 returned an OSL age of 10.7 ± 1 ka (X2730; obtained from the
454 upper sands) implying aggradation during the earliest Holocene and that incision or channel
455 abandonment had probably already occurred as overbank sedimentation had begun. If we
456 assume that sediment exhaustion has not occurred by the early Holocene, and with shifts to
457 cooler, wetter conditions at 11.2, 11.4 and 10.8 ka cal. BP (Barber et al., 2003; Mayewski et al.,
458 2004; Lang et al., 2010; Vincent et al., 2011) recorded in terrestrial, lacustrine and bog surface
459 wetness (BSW) records, it is easy to envisage a situation where paraglacial adjustment remained
460 dominant (Ballantyne, 2005; 2019) and a sediment-dominated fluvial system persisted. The
461 presence of this higher group of terraces (T1-T4) and the Dilston fan (Zone I) suggests the period
462 was dynamic and unstable and that cycles of incision and aggradation during the GS-1 continued
463 into early Holocene period. Comparable responses are evident from the landform sequences of
464 river systems in north Northumberland, the Southern Uplands, central Scotland and the Highlands
465 (Tipping et al., 2008; Passmore and Waddington, 2009, Ballantyne, 2019; Werritty, 2021).

466 5.3. Early to Mid-Holocene

467 Early to mid-Holocene fluvial development is reflected in a single incision and aggradation cycle,
468 leading to the development of T4 and T5. The incision of T4 occurred after 10.7 ± 1 ka (X2730).

469 Although OSL ages were obtained for T5 (X2731, X2732, X2832) the model identified these as

470 outliers and were disregarded. The rationale for this was that the obtained OSL ages were too old

471 and were most likely the result of poor resetting of the OSL signal. Thus, development of T4 and
472 T5 is constrained to the period 8.7 ± 2.3 ka (probability-based time frame). Both T4 and T5 have
473 low sinuosity to straight palaeochannels evident on their surfaces, and the sediments comprise
474 lithofacies assemblages of crudely bedded, imbricated coarse sandy gravels, overlain by a
475 veneer of silty sands. Channel fills within the sequence comprise poorly bedded sands, silty
476 sands and silts, with occasional lenses of coarse boulders and inversely graded sands, thought to
477 represent flooding events. The sediments of T4 and T5 are interpreted as channel bed and bar
478 deposits, channel fills and overbank sedimentation. T4 sequences suggest low aggradation rates
479 and laterally stable channels during the early Holocene, whereas T5 comprises some vertically
480 stacked sequences suggesting periods of instability as we moved towards the mid-Holocene. The
481 early to mid-Holocene landscape was one of increasing stability and soil development, with
482 regional vegetation records indicating that open grasslands and shrubs were replaced by
483 postglacial woodlands (*Juniperus*, *Betula* and *Corylus*) (Innes, 1999; Vincent et al., 2011; Ghilardi
484 and O'Connell, 2013; Innes et al., 2021). Anthropogenic disturbances have been recorded in
485 North Tyne pollen sequences (Moore, 1998) as early as 8.5 ka BP (late Mesolithic), which when
486 combined with recorded cooler and wetter conditions at 8.6–8.2 and 7.8–7.4 ka cal. BP (Barber et
487 al., 2003; Lang et al., 2010; Vincent et al., 2011) may explain the flooding deposits and lateral
488 instability recorded as we move towards the mid-Holocene.

489 5.4. Mid to Late Holocene

490 The mid- to Late Holocene fluvial development is reflected in the lower group of terraces, T5 to
491 T7. An OSL age of 3.2 ± 0.5 ka (X2733) was obtained from overbank sands of T7, and
492 development of T5 – T7 has been constrained to 4.0 ± 1.8 ka (probability-based time frame). T6
493 and T7 dominate zones II and III, however, only T6 is present in zone I and inset below the higher
494 terrace group (T1-T4) and the outwash terraces. Palaeochannels on the surface of T6 indicate
495 low to moderately sinuous channels suggesting development of a wandering-gravel bed system,
496 however, there are several migratory meander bends, evidenced by scroll-bars, indicating
497 channel instability. The sediments of T6 and T7 comprise basal sandy gravels that pass into silty
498 sands and laminated silts. Significant peat-infilled channels and silty peats dominate the upper

499 lithofacies assemblages. These suggest laterally migrating channels, and backwater zones are
500 indicated by the burial of peat-filled channels and slough channels infilled with inverted
501 stratigraphy towards the outer margins of T6. During this period, climatic instability is reflected in
502 increased bog surface wetness (BSW) records at 6.2, 5.7, 5.4, 5.4, 4.4–4.0 ka cal. BP (Hughes et al.,
503 al., 2000; Barber et al., 2003; Charman et al., 2006). Additionally, regional vegetation records
504 (Moores, 1998; Moores et al., 1999) indicate early anthropogenic disturbances in the North Tyne
505 catchment, with significant human activity from the late Mesolithic through to the Neolithic (*cf.*
506 Tolan-Smith, 1996; Waddington and Passmore, 2009). The landscape became largely tree-less,
507 with cultivated pollen taxa and anthropogenic indicator species dominating, especially during the
508 late Bronze Age to Romano-British period. It is easy to envisage periods of widespread fluvial
509 activity driven by increased incidence of flooding, extreme events and channel abandonment in a
510 landscape that was primed (sensitised) by human disturbances and with a paraglacial legacy
511 (Ballantyne, 2005; 2019) providing plentiful erodible sediments. The extent of T6 and T7 (Zones I-
512 III), including the Allen fan (Zone III) reflect major fluvial activity within the catchment, with
513 significant valley floor reworking and probable reincorporation of earlier fluvial deposits but it did
514 not incise into its Lateglacial valley infill (Figs. 5 & 6).

515

516 Passmore and Macklin (2000) present a radiocarbon date of 3.2 ka cal. BP (BETA-45549) for (our)
517 T7, obtained from the South Tyne at Lambley (Fig. 1), however, Passmore and Macklin (1994)
518 also present a radiocarbon date of 5.7 ka cal. BP for (our) T4 and an OSL age of 2.45 ± 3.5 ka for
519 (our) T5, obtained from the Tyne at Farnley Haughs (though discounted for the Bayesian model
520 due to reliability of OSL ages obtained using earlier dating protocols) that raises questions about
521 our chronology. However, there is very little altitudinal separation between T5 and T7 (only 2m),
522 and the terrace long profile (Fig. 3) shows that the surfaces lie closer in elevation downstream
523 and may reflect lateral variability evidenced by the switch to scroll-bars on the surface of T6,
524 rather than significant incision. In addition, sediment deposition at Farnley Haughs occurs in a
525 pinch-point in the valley, potentially allowing higher aggradation at this site compared to the open
526 valley floor setting in the South Tyne at Lambley and Fourstones. Whilst significant

527 improvements in dating protocols (both radiocarbon and OSL) have occurred in the last 30 years
528 (Wintle, 2008; Mahan et al., 2022), we could be seeing a situation of pass-the-parcel sediment
529 movement through depocentres (*sensu* Chiverrell et al., 2010) and a well-ordered younging
530 progression downstream is not present. Using an example from the last 200 years, Passmore and
531 Macklin (2000) have shown that in response to 18th Century metal mining-induced sedimentation
532 and Little Ice Age (LIA) climatic instability the Tyne propagated sediment slugs (*cf.* Nicholas et al.,
533 1995) through its system. The widespread lateral instability in the uplands was subsequently
534 transmitted downstream in a time-transgressive manner.

535

536 The last 3 ka has seen periods of increased instability recorded in river systems throughout
537 northern England (Foster et al., 2009; Chiverrell et al, 2010; Macklin et al., 2014). The results
538 here suggest that there is limited later Holocene activity in the central reaches of the Tyne Valley.
539 Although T8 and T9 are undated, they must be younger than 3.2 ± 0.5 ka based on the OSL age
540 obtained from T7 (X2734). They constitute the least well-developed terraces in the sequence due
541 to their limited extent along the central reaches. Comparable to those recorded in the South Tyne
542 at Lambley (Passmore and Macklin, 2000), they most likely developed during the recent historic
543 period. Early clearance of the Tyne catchment likely explains regional (northern England)
544 variations in fluvial response during this period, driven by the relationship between land-use
545 changes, climatic shifts and flooding episodes. Whilst incision (down to bedrock) is recorded in
546 the tributaries of the South Tyne during last 1.2 ka (Macklin et al., 1992), it appears that there is a
547 disconnect between the uplands (hillslope) and channel after the large depocentres (T6 – T7)
548 developed, and subsequent periods of instability were reflected in lateral channel migration and
549 reach instability, but not in further cut and fill episodes in the central reaches.

550

551 Naturally, the uplands with their connectivity to hillslopes and their fragility in terms of land cover
552 would be more sensitive to external forcing. The response to such forcing is evident in the
553 channel floor activity and incision seen in the upper reaches of the South and North Tyne rivers
554 and their tributaries (Macklin et al., 1992; Moores et al., 1999; Passmore and Macklin, 2000;

555 Macklin and Rumsby, 2007). The fluvial response in the uplands (South Tyne tributaries) has
556 been much more dynamic and sensitive to climatic instabilities and anthropogenic activity
557 (Macklin et al., 1992; Rumsby and Macklin, 1996) during the last 1 ka than that in the central
558 zones in the Tyne Valley corridor, which have been relatively stable since the onset of the later
559 Holocene period. This indicates that major sub-sections of the catchment are not synchronous.
560 Therefore, the upper catchment can be assumed to be more sensitive to change, and that
561 connectivity between the hillslope and the catchment is weaker in the piedmont zone. This
562 suggests that catchment-wide response is diachronous, and it is apparent that the system is
563 operating in discrete, reach-wide responses, such that correlating terraces throughout the whole
564 system is not always possible.

565 **6. Conclusion**

566 This study aimed to reconstruct the alluvial record of the Tyne valley following deglaciation.
567 Through a combination of geomorphological mapping and sedimentological investigations,
568 combined with new OSL ages obtained from fluvial sands, we have been able to present a valley
569 floor history that spans the period following retreat of the TGIS up to the recent historic period.
570

571 The Tyne valley terrace sequence reveals significant alluvial response following deglaciation,
572 resulting in a pattern of incision and valley refilling and leading to the presence of nine alluvial
573 terraces lying between 20 and 2 m (T1 – T9) above present river level. New OSL ages obtained
574 from T1 (12.9 ± 1 ka), T4 (10.7 ± 1 ka) and T7 (3.2 ± 0.5 ka), alongside probability-based modelling
575 bracket terrace development to four phases (i) deglacial phase: 16.0 ± 2.1 ka; proglacial outwash
576 terraces, (ii) Lateglacial phase: 11.9 ± 3.1 ka; high level alluvial terraces T1-T4, (iii) early to mid-
577 Holocene phase: 8.7 ± 2.3 ka; alluvial terraces T4-T5, and (iv) mid- to late Holocene phase: $4.0 \pm$
578 1.8 ka; low level extensive alluvial terraces T5-T7. The later Holocene to recent historic period is
579 reflected by the presence of T8 and T9.

580

581 Development of T1 to T4 was in response to climatic shifts (GI-1, GS-1, and early Holocene
582 events), associated landscape instability and the legacy of glacial inheritance during GS-1 and

583 early Holocene. This is in contrast with previous studies that suggested there was little/no activity
584 during the early Holocene. However, we suggest this was, in part, due to a lack of dated
585 sequences and the lack of high-resolution digital terrain (LiDAR) data to facilitate better
586 identification.

587

588 Significant fluvial activity is recorded during the mid- to late Holocene, with T6 and T7
589 representing a major period of landscape instability and reorganisation. These laterally extensive
590 terraces comprise most of the valley floor sequence, and reflect a period of upland landscape
591 stripping and redistribution driven by increased precipitation due to climatic instability, major
592 anthropogenic disturbances, and a ready supply of easily erodible glacial sediments.
593 Subsequent fluvial activity suggests cannibalisation of earlier terraces, with recent historic activity
594 (T8 and T9) confined to within these dominant terraces (T6 – T7).

595

596 The sedimentary sequence underlying the terraces indicates that incision following deglaciation
597 did not incised through the glacial infill (in the mid-Tyne valley) and there is a clear boundary
598 between those sediments and the Holocene fill. The sediments underlying the terraces reflect
599 transition from a meandering system during the early postglacial phase to a dominant wandering-
600 gravel bed system that persists today.

601

602 This research highlights the importance of catchment-wide investigations and the need for
603 rigorous dating controls. The Tyne valley terrace sequence reflects the importance of complex
604 responses within the fluvial system, and demonstrates that localised responses can temper and
605 impact the broader responses to external climatic drivers. The results are broadly similar to
606 models of fluvial response in other upland UK (Chiverrell et al., 2010) and northern European
607 systems (Vandenderge 2008, 2015) but highlights that the valley floor has been operating in a
608 series of discrete reach-wide responses, and thus, correlation of terraces throughout the whole
609 system is not always possible.

610

611 **Acknowledgements**

612 This paper is based upon work undertaken when LY was in receipt of a University of Hull PhD
613 Scholarship. The two anonymous reviewers are thanked for their positive and constructive
614 comments. OSL dating work was funded by a joint Quaternary Research Association (QRA) and
615 Research Laboratory for Archaeology and History of Art (University of Oxford) Luminescence
616 Dating Award given to LY. We thank the numerous landowners along the Tyne valley for granting
617 access to their land, and CEMEX for access to their quarry sites. LY would like to thank Dr
618 Barbara Rumsby for the continued support and advice over the years. We thank our colleagues
619 for their valuable time, contributions to fieldwork and useful discussions.

620 **References**

- 621 Aitken, M.J., 1985. Thermoluminescence dating: past progress and future trends. *Nuclear Tracks*
622 *and Radiation Measurements* (1982) 10(1–2), 3–6. [https://doi.org/10.1016/0735-](https://doi.org/10.1016/0735-245X(85)90003-1)
623 [245X\(85\)90003-1](https://doi.org/10.1016/0735-245X(85)90003-1)
- 624 Bakke, J., Lie, Ø., Heegaard, E., Dokken, T., Haug, G.H., Birks, H.H., Dulski, P., Nilsen, T., 2009.
625 Rapid oceanic and atmospheric changes during the Younger Dryas cold period. *Nature*
626 *Geoscience* 2, 202–205. <https://doi.org/10.1038/ngeo439>
- 627 Ballantyne, C.K., 2005. Paraglacial Landsystems. In: Evans, D.J.A. (Ed.), *Glacial Landsystems*.
628 Hodder Arnold, London, pp. 432–461.
- 629 Ballantyne, C.K., 2019. After the ice: Lateglacial and Holocene landforms and landscape
630 evolution in Scotland. *Earth and Environmental Science Transactions of the Royal Society*
631 *of Edinburgh* 110(1–2), 33–171. <https://doi.org/10.1017/S175569101800004X>
- 632 Banerjee, D., Murray, A.S., Bøtter-Jensen, L., Lang, A., 2001. Equivalent dose estimation using a
633 single aliquot of polymineral fine grains. *Radiation measurements* 33(1), 73–94.
634 [https://doi.org/10.1016/S1350-4487\(00\)00101-3](https://doi.org/10.1016/S1350-4487(00)00101-3)
- 635 Barber, K.E., Chambers, F.M., Maddy, D., 2003. Holocene palaeoclimates from peat stratigraphy:
636 macrofossil proxy climate records from three oceanic raised bogs in England and Ireland.
637 *Quaternary Science Reviews* 22, 521–539. <https://doi.org/10.1016/S0277-3791>
- 638 Bateman, M.D., Buckland, P.C., Whyte, M.A., Ashurst, R.A., Boulter, C., Panagiotakopulu, E.,
639 2011. Re-evaluation of the Last Glacial Maximum typesite at Dimlington, UK. *Boreas* 40,
640 573–584. <https://doi.org/10.1111/j.1502-3885>
- 641 Bell, W.T., 1979 Attenuation factors for the absorbed radiation dose in quartz inclusions for
642 thermoluminescence dating. *Ancient TL* 8, 1-12.
- 643 Bendle, J.M., Glasser, N.F., 2012. Palaeoclimatic reconstruction from lateglacial (younger dryas
644 chronozone) cirque glaciers in snowdonia, north wales. *Proceedings of the Geologists'*
645 *Association* 123(1), 130–145. <https://doi.org/10.1016/j.pgeola.2011.09.006>
- 646 Blacknell, C., 1981. Sandy gravel accumulation in a fluvial environment. *Geological Journal* 16,
647 287–97. <https://doi.org/10.1002/gj.3350160407>

648 Blacknell, C., 1982. Morphology and surface sedimentary features of point bars in Welsh gravel-
649 bed rivers. *Geological Magazine* 119, 181–192.

650 Bluck, B.J., 1979. Structure of coarse grained braided stream alluvium. *Transactions of the Royal*
651 *Society of Edinburgh* 70, 181–221.

652 Blum, M.D., Törnqvist, T.E., 2000. Fluvial responses to climate and sea-level change: a review
653 and look forward. *Sedimentology* 47, 2–48. <https://doi.org/10.1046/j.1365-3091>

654 Bond, G., Showers, W., Cheseby, M., Lotti, R., Almasi, P., DeMenocal, P., Priore, P., Cullen, H.,
655 Hajdas, I., Bonani, G., 1997. A pervasive millennial-scale cycle in North Atlantic Holocene
656 and glacial climates. *Science* 278(5341), 1257–1266.
657 <https://doi.org/10.1126/science.278.5341.1257>

658 Bøtter-Jensen, L., 1997. Luminescence techniques: instrumentation and methods. *Radiation*
659 *Measurements* 27(5–6), 749–768. [https://doi.org/10.1016/S1350-4487\(97\)00206-0](https://doi.org/10.1016/S1350-4487(97)00206-0)

660 Bøtter-Jensen, L., Bulur, E., Duller, G.A.T., Murray, A.S., 2000. Advances in luminescence
661 instrument systems. *Radiation Measurements* 32(5–6), 523–528.
662 [https://doi.org/10.1016/S1350-4487\(00\)00039-1](https://doi.org/10.1016/S1350-4487(00)00039-1)

663 Bradley S, Milne G, Shennan I, Edwards, R., 2011. An improved Glacial Isostatic Adjustment
664 model for the British Isles. *Journal of Quaternary Science* 26, 541–552.
665 <https://doi.org/10.1002>

666 Bradley, S.L., Ely, J.C., Clark, C.D., Edwards, R.J., Shennan, I., 2023. Reconstruction of the
667 palaeo-sea level of Britain and Ireland arising from empirical constraints of ice extent:
668 implications for regional sea level forecasts and North American ice sheet volume. *Journal*
669 *of Quaternary Science*, 1-15. <https://doi:10.1002/jqs.3523>

670 Brennan, B.J., Lyons, R.G., Phillips, S.W., 1991 Attenuation of alpha particle track dose for
671 spherical grains. *International Journal of Radiation Applications and Instrumentation. Part*
672 *D. Nuclear Tracks and Radiation Measurements* 18, 249-253.

673 Bridge, J. S., 2009. Rivers and floodplains: forms, processes, and sedimentary record. Wiley.

674 Bridgland, D.R., (Ed.), 1986. Clast Lithological Analysis, QRA Technical Guide 3. Quaternary
675 Research Association, London, p. 207.

676 Bridgland, D.R., Westaway, R., Howard, A.J. Innes, J.B., Long, A.J., Mitchell, W.A., White, M.J.,
677 White, T.S., 2010. The role of glacio-isostasy in the formation of post-glacial river terraces
678 in relation to the MIS 2 ice limit: evidence from northern England. *Proceedings of the*
679 *Geologists' Association* 121, 113–127. <https://doi.org/10.1016/j.pgeola.2009.11.004>

680 Brierley, G.J., Hickin, E.J., 1991. Channel planform as a non-controlling factor in fluvial
681 sedimentology: the case of the Squamish River floodplain, British Columbia. *Sedimentary*
682 *Geology* 75(1–2), 67–83. [https://doi.org/10.1016/0037-0738\(91\)90051-E](https://doi.org/10.1016/0037-0738(91)90051-E)

683 Bronk Ramsey, C., 2008. Deposition models for chronological records. *Quaternary Science*
684 *Reviews* 27(1-2), 42-60. <https://doi.org/10.1016/j.quascirev.2007.01.019>

685 Bronk Ramsey, C., 2009. Bayesian analysis of radiocarbon dates. *Radiocarbon* 51(1), 337-360.
686 <https://doi.org/10.1017/S0033822200033865>

687 Bronk Ramsey, C., 2021. OxCal v4. 4.4. Available at: Retrieved from
688 <https://c14.arch.ox.ac.uk/oxcal.html>

689 Brown, A.G., Toms, P.S., Carey, C.J., Howard, A.J.,
689 Challis, K., 2013. Late Pleistocene–Holocene river dynamics at the Trent-Soar confluence,
690 England, UK. *Earth Surface Processes and Landforms* 38(3), 237-
691 249. <https://doi.org/10.1002/esp.3270>

692 Brunsdon, D., Thornes, J.B., 1979. Landscape sensitivity and change. *Transactions of the*
693 *Institute of British Geographers* 4, 463–484. <https://doi.org/10.2307/622210>

694 Buck, C.E., Cavanagh, W.G., Litton, C.D., 1996. Bayesian approach to interpreting archaeological
695 data. Wiley, Chichester, p. 404.

696 Charman, D.J., Blundell, A., Chiverrell, R.C., Hendon, D., Langdon, P.G., 2006. Compilation of
697 non-annually resolved Holocene proxy climate records: stacked Holocene peatland
698 palaeo-water table reconstructions from northern Britain. *Quaternary Science Reviews* 25,
699 336–350. <https://doi.org/10.1016/j.quascirev.2005.05.005>

700 Chiverrell, R.C., Foster, G.C., Marshall, P., Harvey, A.M., Thomas, G.S.P., 2009a. Coupling
701 relationships: Hillslope-fluvial linkages in the Hodder catchment, NW England.
702 *Geomorphology* 109, 222–235. <https://doi.org/10.1016/j.geomorph.2009.03.004>

703 Chiverrell, R.D.C., Foster, G.C., Thomas, G.S.P., Marshall, P., Hamilton, D., 2009b. Robust

704 chronologies for landform development. *Earth Surface Processes and Landforms* 34(2),
705 319-328. <https://doi.org/10.4002/esp.1720>

706 Chiverrell, R.C., Foster, G.C., Thomas, G.S.P., Marshall, P., 2010. Sediment transmission and
707 storage: the implications for reconstructing landform development. *Earth Surface*
708 *Processes and Landforms* 35, 4–15. <https://doi.org/10.1002/esp.1806>

709 Clark, C.D., Ely, J.C., Hindmarsh, R.C., Bradley, S., Ignéczi, A., Fabel, D., Ó Cofaigh, C.,
710 Chiverrell, R.C., Scourse, J., Benetti, S., Bradwell, T., Evans, D.J.A., Roberts, D.H.,
711 Burke, M., Callard, S. L., Medialdea, A., Saher, M., Small, D., Smedley, R.K., Gasson, E.,
712 Gregoire, L., Gandy, N., Hughes, A.L.C., Ballantyne, C., Bateman, M.D., Bigg,
713 G.R., Doole, J., Dayton, D., Duller, G.A.T., Jenkins, G.T.H., Livingstone, S.L., McCarron,
714 S., Moreton, S., Pollard, D., Praeg, D., Sejrup, HP., Van Landeghem, K.J.J., Wilson, P.,
715 2022. Growth and retreat of the last British–Irish Ice Sheet, 31 000 to 15 000 years ago:
716 the BRITICE-CHRONO reconstruction. *Boreas* 51(4), 699-758.
717 <https://doi.org/10.1111/bor.12594>

718 Collins, P.E., Worsley, P., Keith-Lucas, D.M., Fenwick, I.M., 2006. Floodplain environmental
719 change during the Younger Dryas and Holocene in Northwest Europe: Insights from the
720 lower Kennet Valley, south central England. *Palaeogeography, Palaeoclimatology,*
721 *Palaeoecology* 233(1-2), 113-133. <https://doi.org/10.1016/j.palaeo.2005.09.01>

722 Cumming, J.S., 1971. Rockhead relief of southeast Northumberland and the lower Tyne Valley.
723 Department of Geography Seminar Papers No. 18. University of Newcastle upon Tyne.

724 Cumming, J.S., 1977. A descriptive account of the buried rockhead topography of Tyneside. In:
725 Fullerton, B. (Ed.), *North Eastern Studies*. Department of Geography, Newcastle upon
726 Tyne, pp. 57–65.

727 Davies, B.J., Roberts, D.H., Ó Cofaigh, C., Bridgland, D.R., Riding, J., Phillips, E., Teasdale, D.,
728 2009. Interlobate ice-sheet dynamics during the Last Glacial Maximum at Whitburn Bay,
729 County Durham, England. *Boreas* 38, 555–578. [https://doi.org/10.1111/j.1502-](https://doi.org/10.1111/j.1502-3885.2008.00083.x)
730 [3885.2008.00083.x](https://doi.org/10.1111/j.1502-3885.2008.00083.x)

- 731 Desloges, J.R., Church, M., 1987. Channel and floodplain facies in a wandering gravel-bed river.
732 In: Ethridge, F.G., Flores, R.M., Harvey, M.D. (Eds.), Recent Developments in Fluvial
733 Sedimentology. Society of Economic Paleontologists and Mineralogists, Special
734 Publication 39, Oklahoma, USA, pp. 99–109.
- 735 Durcan, J.A., King, G.E., Duller, G.A.T., 2015 DRAC: Dose rate and age calculator for trapped
736 charge dating. *Quaternary Geochronology* 28, 54-61.
737 <https://doi.org/10.1016/j.quageo.2015.03.012>
- 738 Evans, I.S., 1999. Castle Eden Dene and Blunts Dene. In: Bridgland, D.R., Horton, B.P., Innes,
739 J.B. (Eds.), The Quaternary of North-East England, QRA Field Guide, Quaternary
740 Research Association, London, pp. 57–63.
- 741 Evans, D.J., Roberts, D.H., Bateman, M.D., Clark, C.D., Medialdea, A., Callard, L., Grimoldi, E.,
742 Chiverrell, R.C., Ely, J., Dove, D., Ó Cofaigh, C., 2021. Retreat dynamics of the eastern
743 sector of the British–Irish Ice Sheet during the last glaciation. *Journal of Quaternary*
744 *Science* 36(5), 723-751. <https://doi:10.1002/jqs.3275>
- 745 Ferguson, R.I., Werritty, A., 1983. Bar development and channel changes in the gravelly River
746 Feshie, Scotland. In: Collinson, J.D., Lewin, J. (Eds.), Modern and Ancient Fluvial
747 Systems, Special Publication of the International Association of Sedimentologists 6.
748 Blackwell, Oxford, pp. 181–193. <https://doi.org/10.1002/9781444303773.ch14>
- 749 Forbes, D.L., 1983. Morphology and sedimentology of a sinuous gravel-bed channel system:
750 lower Babbage River, Yukon coastal plain, Canada. In: Collinson, J.D., Lewin, J. (Eds.),
751 Modern and Ancient Fluvial Systems, Special Publication of the International Association
752 of Sedimentologists 6. Blackwell, Oxford, pp. 195–206.
753 <https://doi.org/10.1002/9781444303773.ch15>
- 754 Foster, G.C., Chiverrell, R.C., Thomas, G.S.P., Marshall, P., Hamilton, D., 2009. Fluvial
755 development and the sediment regime of the lower Calder, Ribble catchment, northwest
756 England. *Catena* 77, 81–95. <https://doi.org/10.1016/j.catena.2008.09.006>
- 757 Fryirs, K.A., 2017. River sensitivity: a lost foundation concept in fluvial geomorphology. *Earth*
758 *Surface Processes and Landforms* 42(1), 55–70. <https://doi.org/10.1002/esp.3940>

- 759 Galbraith, R.F., Laslett, G.M., 1993. Statistical models for mixed fission track ages. *Nuclear tracks*
760 *and radiation measurements* 21(4), 459–470. [https://doi.org/10.1016/1359-](https://doi.org/10.1016/1359-0189(93)90185-C)
761 [0189\(93\)90185-C](https://doi.org/10.1016/1359-0189(93)90185-C)
- 762 Galbraith, R.F., Roberts, R.G., Laslett, G.M., Yoshida, H., Olley, J.M., 1999. Optical dating of
763 single and multiple grains of quartz from Jinmium rock shelter, northern Australia: Part I,
764 experimental design and statistical models. *Archaeometry* 41(2), 339–364.
765 <https://doi.org/10.1111/j.1475-4754.1999.tb00988.x>
- 766 Gao, C., Boreham, S., Preece, R.C., Gibbard, P.L., Briant, R.M., 2007. Fluvial response to rapid
767 climate change during the Devensian (Weichselian) Lateglacial in the River Great Ouse,
768 southern England, UK. *Sedimentary Geology* 202(1-2), 193-210.
769 <https://doi.org/10.1016/j.sedgeo.2007.02.004>
- 770 Ghilardi, B., O'Connell, M., 2013. Early Holocene vegetation and climate dynamics with particular
771 reference to the 8.2 ka event: pollen and macrofossil evidence from a small lake in
772 western Ireland. *Vegetation history and archaeobotany* 22, 99–114.
773 <https://doi.org/10.1007/s00334-012-0367-x>
- 774 Gibbard, P.L., Lewin, J., 2002. Climate and related controls on interglacial fluvial sedimentation in
775 lowland Britain. *Sedimentary Geology* 151(3–4), 187–210. [https://doi.org/10.1016/S0037-](https://doi.org/10.1016/S0037-0738(01)00253-6)
776 [0738\(01\)00253-6](https://doi.org/10.1016/S0037-0738(01)00253-6)
- 777 Golledge, N.R., 2010. Glaciation of Scotland during the Younger Dryas stadial: a review. *Journal*
778 *of Quaternary Science* 25, 550–566. <https://doi.org/10.1002/jqs.1319>
- 779 Guérin, G., Mercier, N., Adamiec, G., 2011. Dose-rate conversion factors: update. *Ancient*
780 *TL* 29(1), 5–8.
- 781 Guérin, G., Mercier, N., Nathan, R., Adamiec, G., Lefrais, Y., 2012. On the use of the infinite
782 matrix assumption and associated concepts: A critical review. *Radiation Measurements*
783 47, 778-785. <https://doi.org/10.1016/j.radmeas.2012.04.004>
- 784 Harrison, S., Bailey, R.M., Anderson, E., Arnold, L., Douglas, T., 2010. Optical Dates from British
785 Isles 'Solifluction Sheets' Suggests Rapid Landscape Response to Late Pleistocene

786 Climate Change. *Scottish Geographical Journal* 126, 101–111.
787 <https://doi.org/10.1080/14702541003712911>

788 Harrison, S., Hughes, L., Glasser, N., Kuras, O., 2021. Late Quaternary solifluction sheets in the
789 British uplands. *Journal of Quaternary Science* 36(7), 1162–1173.
790 <https://doi.org/10.1002/jqs.3369>

791 Harvey, A.M., Renwick, W.H., 1987. Holocene alluvial fan and terrace formation in the Bowland
792 Fells Northwest England. *Earth Surface Processes and Landforms* 12, 249–
793 257. <https://doi.org/10.1002/esp.3290120304>

794 Hill, T.C., Woodland, W.A., Spencer, C.D., Marriott, S.B., Case, D.J. and Catt, J.A., 2008.
795 Devensian late-glacial environmental change in the Gordano Valley, North Somerset,
796 England: a rare archive for southwest Britain. *Journal of paleolimnology* 40, 431-444.

797 Hooke, J., 2003. River meander behaviour and instability: a framework for analysis. *Transactions*
798 *of the Institute of British Geographers* 28, 238–253. [https://doi.org/10.1111/1475-](https://doi.org/10.1111/1475-5661.00089)
799 [5661.00089](https://doi.org/10.1111/1475-5661.00089)

800 Hooke, J. M., 2004. Cutoffs galore!: occurrence and causes of multiple cutoffs on a meandering
801 river. *Geomorphology* 61, 225–238. <https://doi.org/10.1016/j.geomorph.2003.12.006>

802 Horton, B.P., Innes, J.B., Shennan, I., 1999a. Late Devensian and Holocene relative sea-level
803 changes in Northumberland, England. In: Bridgland, D.R., Horton, B.P., Innes, J.B. (Eds.),
804 The Quaternary of North-East England, QRA Field Guide. Quaternary Research
805 Association, London, pp. 35–47.

806 Horton, B.P., Innes, J.B., Plater, A.J., Tooley, M.J., Wright, M.R., 1999b. Post-glacial evolution
807 and relative sea-level changes in Hartlepool Bay and the Tees estuary. In: Bridgland,
808 D.R., Horton, B.P., Innes, J.B. (Eds.), The Quaternary of North-East England, QRA Field
809 Guide. Quaternary Research Association, London, pp. 65–86.

810 Howard, A.J., Carney, J.N., Greenwood, M.T., Keen, D.H., Mighall, T., O'Brien, C. and Tetlow, E.,
811 2011. The Holme Pierrepont sand and gravel and the timing of Middle and Late
812 Devensian floodplain aggradation in the English Midlands. *Proceedings of the Geologists'*
813 *Association* 122(3), 419-431.

814 Howard, A.J., Macklin, M.G., Black, S., Hudson-Edwards, K.A., 2000a. Holocene river
815 development and environmental change in Upper Wharfedale, Yorkshire Dales,
816 England. *Journal of Quaternary Science* 15(3), 239–252.
817 [https://doi.org/10.1002/\(SICI\)1099-1417\(200003\)15:3<239::AID-JQS480>3.0.CO;2-W](https://doi.org/10.1002/(SICI)1099-1417(200003)15:3<239::AID-JQS480>3.0.CO;2-W)

818 Howard, A.J., Keen, D.H., Mighall, T.M., Field, M.H., Coope, G.R., Griffiths, H.I., Macklin, M.G.,
819 2000b. Early Holocene environments of the River Ure near Ripon, North Yorkshire,
820 UK. *Proceedings of the Yorkshire Geological Society* 53(1), 31–41.

821 Hughes, A. L., Clark, C. D., Jordan, C. J. 2014. Flow-pattern evolution of the last British Ice
822 Sheet. *Quaternary Science Reviews* 89, 148–168.
823 <https://doi.org/10.1016/j.quascirev.2014.02.002>

824 Hughes, P.D., Clark, C.D., Gibbard, P.L., Glasser, N.F., Tomkins, M.D., 2023. Britain and Ireland:
825 glacial landforms during deglaciation. In: Palacios, D., Hughes, P.D., García-Ruiz, J.,
826 Andrés, N. (Eds.), *European Glacial Landscapes, The Last Deglaciation*. Elsevier,
827 London, pp. 129–139. <https://doi.org/10.1016/B978-0-323-91899-2.00027-9>

828 Hughes, P.D.M., Mauquoy, D., Barber, K.E., Langdon, P.G., 2000. Mire-development pathways
829 and palaeoclimatic records from a full Holocene peat archive at Walton Moss, Cumbria,
830 England. *The Holocene* 10, 465–479. <https://doi.org/10.1016/j.quascirev.2014.02.002>

831 Innes, J.B., 1999. Regional Vegetational History. In: Bridgland, D.R., Horton, B.P., Innes, J.B.
832 (Eds.), *The Quaternary of North-East England, QRA Field Guide*. Quaternary Research
833 Association, Cambridge, pp. 21–34.

834 Innes, J., Mitchell, W., O'brien, C., Roberts, D., Rutherford, M., Bridgland, D., 2021. A Detailed
835 Record of Deglacial and Early Post-Glacial Fluvial Evolution: The River Ure in North
836 Yorkshire, UK. *Quaternary* 4(1), p. 9. <https://doi.org/10.3390/quat4010009>

837 Johnson, G.A.L., 1997. Geology of Hadrian's Wall. *Geologists' Association Guide* 59. Geologists'
838 Association, London, p. 89.

839 Jones, A.P., Tucker, M.E., Hart, J.K., 1999. The Description and Analysis of Quaternary
840 Stratigraphic Field Sections. *QRA Technical Guide* 7. Quaternary Research Association,
841 London. p. 286.

842 Kreutzer, S., Schmidt, C., Fuchs, M.C., Dietze, M., Fischer, M. and Fuchs, M. 2012 Introducing an
843 R package for luminescence dating analysis. *Ancient TL* 30, pp. 1-8

844 Lang, B., Bedford, A., Brooks, S.J., Jones, R.T., Richardson, N., Birks, H. J.B., Marshall, J.D.
845 2010. Early-Holocene temperature variability inferred from chironomid assemblages at
846 Hawes Water, northwest England. *The Holocene* 20, 943–954.
847 <https://doi.org/10.1177/0959683610366157>

848 Lewin, J., Gibbard, P.L., 2010. Quaternary river terraces in England: forms, sediments and
849 processes. *Geomorphology*, 120(3-4), 293-311.
850 <https://doi.org/10.1016/j.geomorph.2010.04.002>

851 Lewin, J., Macklin, M.G., 2003. Preservation potential for Late Quaternary river alluvium. *Journal*
852 *of Quaternary Science* 18, 107–120. <https://doi.org/10.1002/jqs.738>

853 Lewin, J., Macklin, M.G., Johnstone, E., 2005. Interpreting alluvial archives: sedimentological
854 factors in the British Holocene fluvial record. *Quaternary Science Reviews* 24, 1873–1889.
855 <https://doi.org/10.1016/j.quascirev.2005.01.009>

856 Livingstone, S.J., Evans, D.J., Cofaigh, C.Ó., Davies, B.J., Merritt, J.W., Huddart, D., Mitchell,
857 W.A., Roberts, D.H., Yorke, L. 2012. Glaciodynamics of the central sector of the last
858 British–Irish Ice Sheet in Northern England. *Earth-Science Reviews* 111, 25–55.
859 <https://doi.org/10.1016/j.earscirev.2011.12.006>

860 Livingstone, S.J., Roberts, D.H., Davies, B.J., Evans, D.J., Ó Cofaigh, C., Gheorghiu, D.M., 2015.
861 Late Devensian deglaciation of the Tyne Gap Palaeo-Ice stream, northern
862 England. *Journal of Quaternary Science* 30(8), 790–804. <https://doi.org/10.1002/jqs.2813>

863 Lowe, J.J., Rasmussen, S.O., Björck, S., Hoek, W.Z., Steffensen, J.P., Walker, M.J.C., Yu, Z.C.,
864 2008. Synchronisation of palaeoenvironmental events in the North Atlantic region during
865 the last termination: a revised protocol recommended by the INTIMATE group.
866 *Quaternary Science Reviews* 27, 6–17. <https://doi.org/10.1016/j.quascirev.2007.09.016>

867 Macklin, M.G., 1999. Holocene river environments in prehistoric Britain: human interaction and
868 impact. *Journal of Quaternary Science* 14, 521–530. [https://doi.org/10.1002/\(SICI\)1099-1417\(199910\)14:6<521::AID-JQS487>3.0.CO;2-G](https://doi.org/10.1002/(SICI)1099-1417(199910)14:6<521::AID-JQS487>3.0.CO;2-G)

869

- 870 Macklin, M.G., Lewin, J., 1993. Holocene river alluviation in Britain. *Zeitschrift für*
871 *Geomorphologie* 47, 109–122.
- 872 Macklin, M.G., Lewin, J., Jones, A.F., 2013. River entrenchment and terrace formation in the UK
873 Holocene. *Quaternary Science Reviews* 76, 194–206.
874 <https://doi.org/10.1016/j.quascirev.2013.05.026>
- 875 Macklin, M.G., Lewin, J., Jones, A.F., 2014. Anthropogenic alluvium: An evidence-based meta-
876 analysis for the UK Holocene, *Anthropocene* 6, 26–38.
877 <https://doi.org/10.1016/j.ancene.2014.03.003>
- 878 Macklin, M.G., Rumsby, B.T., 2007. Changing climate and extreme floods in the British
879 uplands. *Transactions of the Institute of British Geographers* 32(2), 68–186.
880 <https://doi.org/10.1111/j.1475-5661.2007.00248.x>
- 881 Macklin, M.G., Rumsby, B.T., Heap, T., 1992. Flood alluviation and entrenchment: Holocene
882 valley-floor development and transformation in the British uplands. *Geological Society of*
883 *America Bulletin* 104(6), 631–643. [https://doi.org/10.1130/0016-](https://doi.org/10.1130/0016-7606(1992)104<0631:FAAEHV>2.3.CO;2)
884 [7606\(1992\)104<0631:FAAEHV>2.3.CO;2](https://doi.org/10.1130/0016-7606(1992)104<0631:FAAEHV>2.3.CO;2)
- 885 Mahan, S.A., Rittenour, T.M., Nelson, M.S., Atae, N., Brown, N., DeWitt, R., Durcan, J., Evans,
886 M., Feathers, J., Frouin, M. and Guérin, G., 2023. Guide for interpreting and reporting
887 luminescence dating results. *GSA Bulletin* 135(5-6), 1480-1502.
888 <https://doi.org/10.1130/B36404.1>
- 889 Mayewski, P.A., Rohling, E.E., Stager, J.C., Karlen, W., Maasch, K.A., Meeker, L.D., Meyerson,
890 E.A., Gasse, F., van Kreveld, S., Holmgren, K., Lee-Thorp, J., Rosqvist, G., Rack, F.,
891 Staubwasser, M., Schneider, R.R., Steig, E.J., 2004. Holocene climate variability.
892 *Quaternary Research* 62, 243–255. <https://doi.org/10.1016/j.yqres.2004.07.001>
- 893 Mejdahl, V., 1979. Thermoluminescence dating: beta-dose attenuation in quartz
894 grains. *Archaeometry* 21(1), 61–72.
- 895 Miall, A.D., 1988. Facies architecture in clastic sedimentary basins. In: Kleinspehn, K.L., Paolo, C.
896 (Eds.) *New perspectives in basin analysis*. *Frontiers in Sedimentary Geology*. Springer,
897 New York, pp. 67–81.

- 898 Miall, A.D. 1996. The Geology of Fluvial Deposits: Sedimentary Facies, Basin Analysis and
899 Petroleum Geology. Springer-Verlag, Berlin, p. 582. [https://doi.org/10.1007/987-3-662-](https://doi.org/10.1007/987-3-662-03237-4)
900 [03237-4](https://doi.org/10.1007/987-3-662-03237-4)
- 901 Mills, D.A.C., Holliday, D.W., 1998. Geology of the district around Newcastle upon Tyne,
902 Gateshead and Consett: Memoir for the 1: 50,000 Geological Sheet 20. HMSO, London,
903 p. 162.
- 904 Mol, J., Vandenberghe, J., Kasse, C., 2000. River response to variations of periglacial climate in
905 mid-latitude Europe. *Geomorphology* 33(3–4), 131–148. [https://doi.org/10.1016/S0169-](https://doi.org/10.1016/S0169-555X(99)00126-9)
906 [555X\(99\)00126-9](https://doi.org/10.1016/S0169-555X(99)00126-9)
- 907 Moores, A.J., 1998. Palaeoenvironmental investigations of Holocene landscapes in the North
908 Tyne basin, northern England. Unpublished PhD thesis, Newcastle University.
909 <http://theses.ncl.ac.uk/jspui/handle/10443/2211>
- 910 Moores, A.J., Passmore, D.G., Stevenson, A.C., 1999. High resolution palaeochannel records of
911 Holocene valley floor environments in the North Tyne basin, northern England. In: Brown,
912 A.G., Brown, A., Quine, T. (Eds.). *Fluvial processes and environmental change* (Vol. 13).
913 Wiley-Blackwell, Chichester, pp. 283–310.
- 914 Murray, A.S., Olley, J.M., Caitcheon, G.G. 1995. Measurement of equivalent doses in quartz from
915 contemporary water-lain sediments using optically stimulated luminescence. *Quaternary*
916 *Science Reviews* 14, 365–371.
- 917 Murray, A.S, Wintle, A.G., 2000. Luminescence dating of quartz using an improved single-aliquot
918 regenerative-dose protocol. *Radiation measurements* 32(1), 57–73.
919 [https://doi.org/10.1016/S1350-4487\(99\)00253-X](https://doi.org/10.1016/S1350-4487(99)00253-X)
- 920 Nesje, A., Lie, Ø., Dahl, S.O., 2000. Is the North Atlantic Oscillation reflected in Scandinavian
921 glacier mass balance records? *Journal of Quaternary Science* 15(6), 587–601.
922 [https://doi.org/10.1016/S0277-3791\(99\)00090-6](https://doi.org/10.1016/S0277-3791(99)00090-6)
- 923 Notebaert, B., Verstraeten, G., 2010. Sensitivity of West and Central European river systems to
924 environmental changes during the Holocene: A review. *Earth-Science Reviews* 103(3–4),
925 163–182. <https://doi.org/10.1016/j.earscirev.2010.09.009>

926 Passmore, D.G., Macklin, M.G., 1994. Provenance of fine-grained alluvium and late Holocene
927 land-use change in the Tyne basin, northern England. *Geomorphology* 9(2), 127–142.
928 [https://doi.org/10.1016/0169-555X\(94\)90071-X](https://doi.org/10.1016/0169-555X(94)90071-X)

929 Passmore, D.G., Macklin, M.G., 2000. Late Holocene channel and floodplain development in a
930 wandering gravel-bed river: the River South Tyne at Lambley, Northern England. *Earth*
931 *Surface Processes and Landforms* 25, 1237–1256. [https://doi.org/10.1002/1096-
932 9837\(200010\)25:11<1237::AID-ESP134>3.0.CO;2-S](https://doi.org/10.1002/1096-9837(200010)25:11<1237::AID-ESP134>3.0.CO;2-S)

933 Passmore, D.G., Waddington, C., 2009. Paraglacial adjustment of the fluvial system to Late
934 Pleistocene deglaciation: the Milfield Basin, northern England. Geological Society,
935 London. Special Publications 320(1),145–164. <https://doi.org/10.1144/SP320.10>

936 Peel, R.F., 1941. The North Tyne Valley. *The Geographical Journal* 98, 5–19.

937 Philips, J.D., 2010. Amplifiers, filters and geomorphic responses to climate change in Kentucky
938 rivers. *Climate Change* 103, 571–595. <https://doi.org/10.1007/s10584-009-9775-z>

939 Pope, A., 2017. SRTM shaded relief DEM of Great Britain, [Dataset]. University of Edinburgh.
940 <https://doi.org/10.7488/ds/1722>

941 Rasmussen, S.O., Bigler, M., Blockley, S.P., Blunier, T., Buchardt, S.L., Clausen, H.B.,
942 Cvijanovic, I., Dahl-Jensen, D., Johnsen, J.L., Fischer, H., Gkinis, V., Guillevic, M., Hoek,
943 W.Z., Lowe, J.J., Pedro, J.B., Popp, T., Seierstad, I.K., Steffensen, J.P., Svensson, A.M.,
944 Vallengø, P., Vinther, B.M., Walker, M.J.C., Wheatley, J.J., Winstrup, M., 2014. A
945 stratigraphic framework for abrupt climatic changes during the Last Glacial period based
946 on three synchronized Greenland ice-core records: refining and extending the INTIMATE
947 event stratigraphy. *Quaternary Science Reviews* 106, 14–28.
948 <https://doi.org/10.1016/j.quascirev.2014.09.007>

949 Reimer, P.J., Austin, W.E., Bard, E., Bayliss, A., Blackwell, P.G., Ramsey, C.B., Butzin, M.,
950 Cheng, H., Edwards, R.L., Friedrich, M., Grootes, P.M., 2020. The IntCal20 Northern
951 Hemisphere radiocarbon age calibration curve (0–55 cal kBP). *Radiocarbon* 62(4),725-
952 757. <https://doi:10.1017/RDC.2020.41>

953 Rice, S.P., Church, M., Wooldridge, C.L., Hickin, E.J., 2009. Morphology and evolution of bars in
954 a wandering gravel-bed river; lower Fraser river, British Columbia, Canada.
955 *Sedimentology* 56, 709–736. <https://doi.org/10.1111/j.1365-3091.2008.00994.x>

956 Rice, S. P., Church, M., 2010. Grain-size sorting within river bars in relation to downstream fining
957 along a wandering channel. *Sedimentology* 57, 232–251. [https://doi.org/10.1111/j.1365-](https://doi.org/10.1111/j.1365-3091.2009.01108.x)
958 [3091.2009.01108.x](https://doi.org/10.1111/j.1365-3091.2009.01108.x)

959 Roberts, D.H., Evans, D.J., Callard, S.L., Clark, C.D., Bateman, M.D., Medialdea, A., Dove, D.,
960 Cotterill, C.J., Saher, M., Cofaigh, C.Ó., Chiverrell, R.C., 2018. Ice marginal dynamics of
961 the last British-Irish Ice Sheet in the southern North Sea: Ice limits, timing and the
962 influence of the Dogger Bank. *Quaternary Science Reviews* 198, 181–207.
963 <https://doi.org/10.1016/j.quascirev.2018.08.010>

964 Rumsby, B. T., Macklin, M. G., 1996. River response to the last neoglacial (the ‘Little Ice Age’) in
965 northern, western and central Europe. Geological Society, London, Special Publications
966 115, 217–233.

967 Scrutton, C.T., 1995. Northumbria Rocks and Landscape. Ellenbank, Leeds, p. 216.

968 Shakun, J.D., Carlson, A.E. 2010. A global perspective on Last Glacial Maximum to Holocene
969 climate change. *Quaternary Science Reviews* 29, 1801–1816.
970 <https://doi.org/10.1016/j.quascirev.2010.03.016>

971 Shennan, I., Bradley, S.L., Edwards, R., 2018. Relative sea-level changes and crustal
972 movements in Britain and Ireland since the Last Glacial Maximum. *Quaternary Science*
973 *Reviews* 188, 143-159. <https://doi.org/10.1016/j.quascirev.2018.03.031>

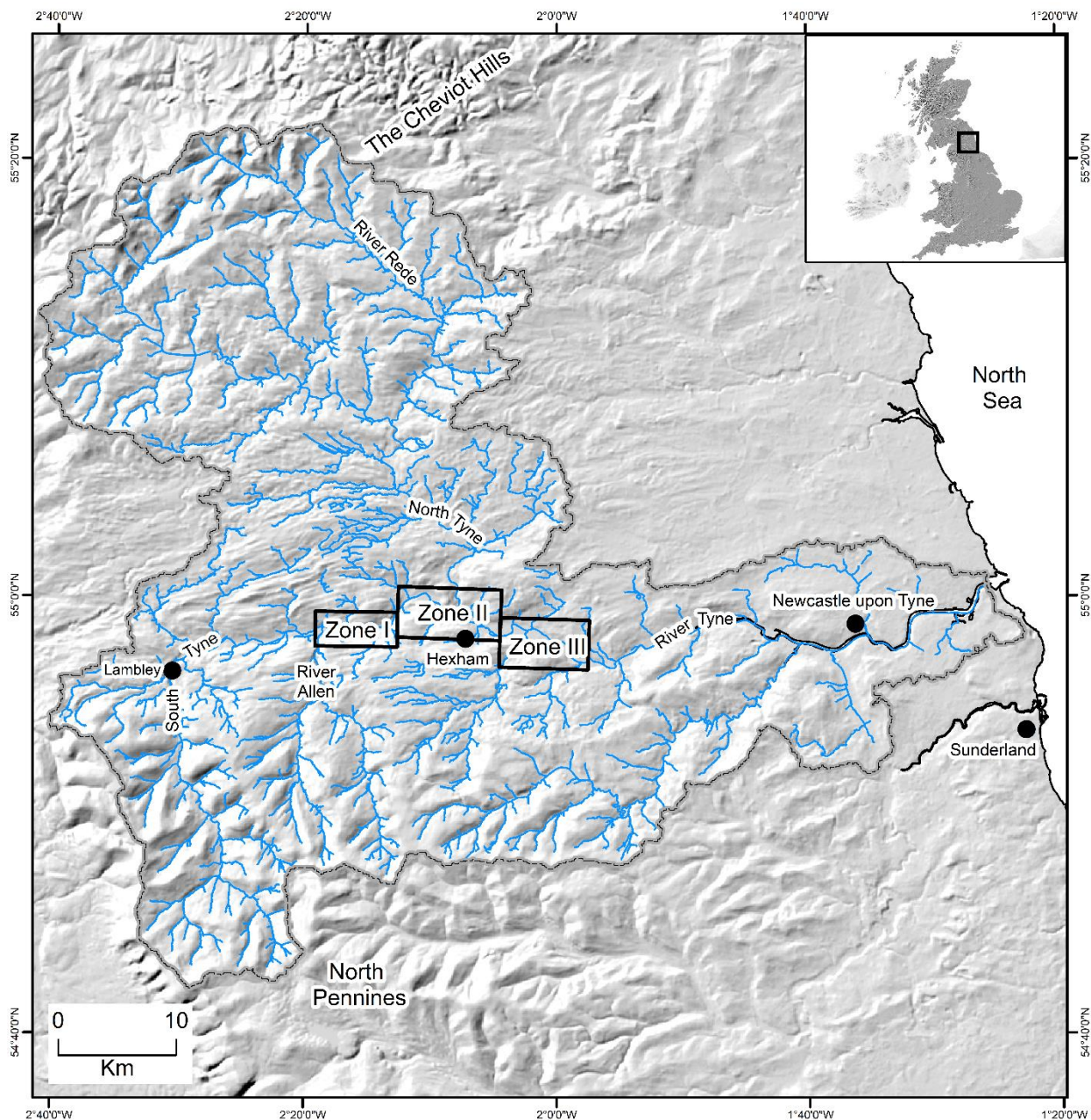
974 Smith, D.B., 1994. Geology of the district around Sunderland. Memoir of the British Geological
975 Survey Sheet 21. HMSO, London, p. 173.

976 Smith, S.A., 1990. The sedimentology and accretionary styles of an ancient gravel bed stream:
977 the Budleigh Salterton Pebble beds (Lower Triassic), southwest England. *Sedimentary*
978 *Geology* 67, 199–219. [https://doi.org/10.1016/0037-0738\(90\)90035-R](https://doi.org/10.1016/0037-0738(90)90035-R)

- 979 Smith, G.H.S., Ashworth, P.J., Best, J.L., Lunt, I.A., Orfeo, O., Parsons, D.R., 2009. The
980 sedimentology and alluvial architecture of a large braid bar, Río Paraná, Argentina.
981 *Journal of Sedimentary Research* 79, 629–642. <https://doi.org/10.2110/jsr.2009.066>
- 982 Teasdale D. 2013. Evidence for the western limits of the North Sea Lobe of the BHS in North East
983 England. In: QRA Field Guide: The Quaternary of Northumberland, Durham and
984 Yorkshire, BJ Davies, B.J., Yorke, L., Bridgland, D.R., Roberts, D.H. (Eds). Quaternary
985 Research Association, Cambridge, pp. 106–121.
- 986 Thornalley, D.J., Elderfield, H., McCave, I.N., 2009. Holocene oscillations in temperature and
987 salinity of the surface subpolar North Atlantic. *Nature* 457, 711–714.
988 <https://doi.org/10.1038/nature07717>
- 989 Thrasher, I., Mauz, B., Chiverrell, R.C., Lang, A., 2009. Luminescence dating of glaciofluvial
990 deposits: A review. *Earth Science Reviews* 97, 133–146.
991 <https://doi.org/10.1016/j.earscirev.2009.09.001>
- 992 Tipping, R., 1994. Fluvial chronology and valley floor evolution of the upper Bowmont valley,
993 Borders Region, Scotland. *Earth surface processes and landforms* 19(7), 641-657.
- 994 Tipping, R., 1995. Holocene evolution of a lowland Scottish landscape: Kirkpatrick Fleming. Part I,
995 peat-and pollen-stratigraphic evidence for raised moss development and climatic
996 change. *The Holocene* 5(1), 69-81.
- 997 Tipping, R.M., Jones, A.P., Carter, S., Holden, T., Cressey, M., 2008. The chronology and long
998 term dynamics of a low energy river system: the Kelvin Valley, central Scotland. *Earth*
999 *Surface Processes and Landforms* 33, 910–922. <https://doi.org/10.1002/esp.158>
- 1000 Tipping, R.M., Milburn, P., Halliday, S., 1999. Fluvial processes, land use and climate change
1001 2000 years ago in upper Annandale, southern Scotland. In: Brown, A.G., Quine, T.A.
1002 (Eds). *Fluvial Processes and Environmental Change*. John Wiley & Sons, Chichester, pp.
1003 311-327.
- 1004 Tolan-Smith, C., 1996. The Mesolithic/Neolithic transition in the North Tyne Valley: a landscape
1005 approach. *Neolithic Studies in No-Man's Land: Papers on the Neolithic of Northern*
1006 *England from the Trent to the Tweed*. *Northern Archaeology* 13(14), 7-16.

- 1007 Tucker, M.E., 2011. Sedimentary Rocks in the Field. The Geological Field Guide Series, 4th Ed.
1008 Wiley, Chichester, p. 229.
- 1009 Vandenberghe, J., 2008. The fluvial cycle at cold–warm–cold transitions in lowland regions: a
1010 refinement of theory. *Geomorphology* 98(3–4), 275–284.
1011 <https://doi.org/10.1016/j.geomorph.2006.12.030>
- 1012 Vandenberghe, J., 2015. River terraces as a response to climatic forcing: formation processes,
1013 sedimentary characteristics and sites for human occupation. *Quaternary International* 370,
1014 3–11. <https://doi.org/10.1016/j.quaint.2014.05.046>
- 1015 van de Lageweg, W.I., van Dijk, W.M., Baar, A.W., Rutten, J., Kleinhans, M.G., 2014. Bank pull or
1016 bar push: What drives scroll-bar formation in meandering rivers? *Geology* 42, 319–322.
1017 <https://doi.org/10.1130/G35192.1>
- 1018 Vincent, P.J., Lord, T.C., Telfer, M.W., Wilson, P., 2011. Early Holocene loessic colluviation in
1019 northwest England: new evidence for the 8.2 ka event in the terrestrial record? *Boreas* 40,
1020 105–115. <https://doi.org/10.1111/j.1502-3885.2010.00172.x>
- 1021 Werritty, A., 2021. Fluvial Landforms of Glen Feshie and the Spey Drainage Basin. In: Ballantyne,
1022 C.K., Gordon, J.E. (Eds) Landscapes and Landforms of Scotland. World
1023 Geomorphological Landscapes. Springer, Cham. pp. 349–358.
1024 https://doi.org/10.1007/978-3-030-71246-4_19
- 1025 Whiting, P.J., Dietrich, W.E., Leopold, L.B., Drake, T.G., Shreve, R.L., 1988. Bedload sheets in
1026 heterogeneous sediment. *Geology* 16, 105–108. [https://doi.org/10.1130/0091-7613\(1988\)016<0105:BSIHS>2.3.CO;2](https://doi.org/10.1130/0091-7613(1988)016<0105:BSIHS>2.3.CO;2)
- 1027
- 1028 Wilson, P., 2002. Morphology and significance of some Loch Lomond Stadial moraines in the
1029 south-central Lake District, England. *Proceedings of the Geologists' Association* 113, 9–
1030 21. [https://doi.org/10.1016/S0016-7878\(02\)80002-5](https://doi.org/10.1016/S0016-7878(02)80002-5)
- 1031 Wintle, A.G., 2008. Fifty years of luminescence dating. *Archaeometry* 50(2), pp.276-312.
1032 <https://doi.org/10.1111/j.1475-4754.2008.00392.x>
- 1033 Wintle, A.G., Murray, A.S., 2006. A review of quartz optically stimulated luminescence
1034 characteristics and their relevance in single-aliquot regeneration dating

- 1035 protocols. *Radiation measurements* 41(4), 369–391.
- 1036 <https://doi.org/10.1016/j.radmeas.2005.11.001>
- 1037 Wooldridge, C.L., Hickin, E.J., 2005. Radar architecture and evolution of channel bars in
1038 wandering gravel-bed rivers: Fraser and Squamish rivers, British Columbia, Canada.
1039 *Journal of Sedimentary Research* 75, 844–860. <https://doi.org/10.2110/jsr.2005.066>
- 1040 Yorke, L., 2008. Late Quaternary Valley Fill Sediments in the River Tyne Valley: Understanding
1041 Late Devensian Deglaciation and Early Postglacial Response in Northern England.
1042 Unpublished Ph.D. thesis, University of Hull. [https://hull-](https://hull-repository.worktribe.com/output/4209010)
1043 [repository.worktribe.com/output/4209010](https://hull-repository.worktribe.com/output/4209010)
- 1044 Yorke, L., Rumsby, B.T., Chiverrell, R.C., 2012. Depositional history of the Tyne valley associated
1045 with retreat and stagnation of Late Devensian Ice Streams. *Proceedings of the Geologists'*
1046 *Association* 123, 608–625. <https://doi.org/10.1016/j.pgeola.2012.03.005>
- 1047 Zimmerman, J., 1971. The radiation-induced increase of the 100 C thermoluminescence
1048 sensitivity of fired quartz. *Journal of Physics C: Solid State Physics* 4(18), 3265.

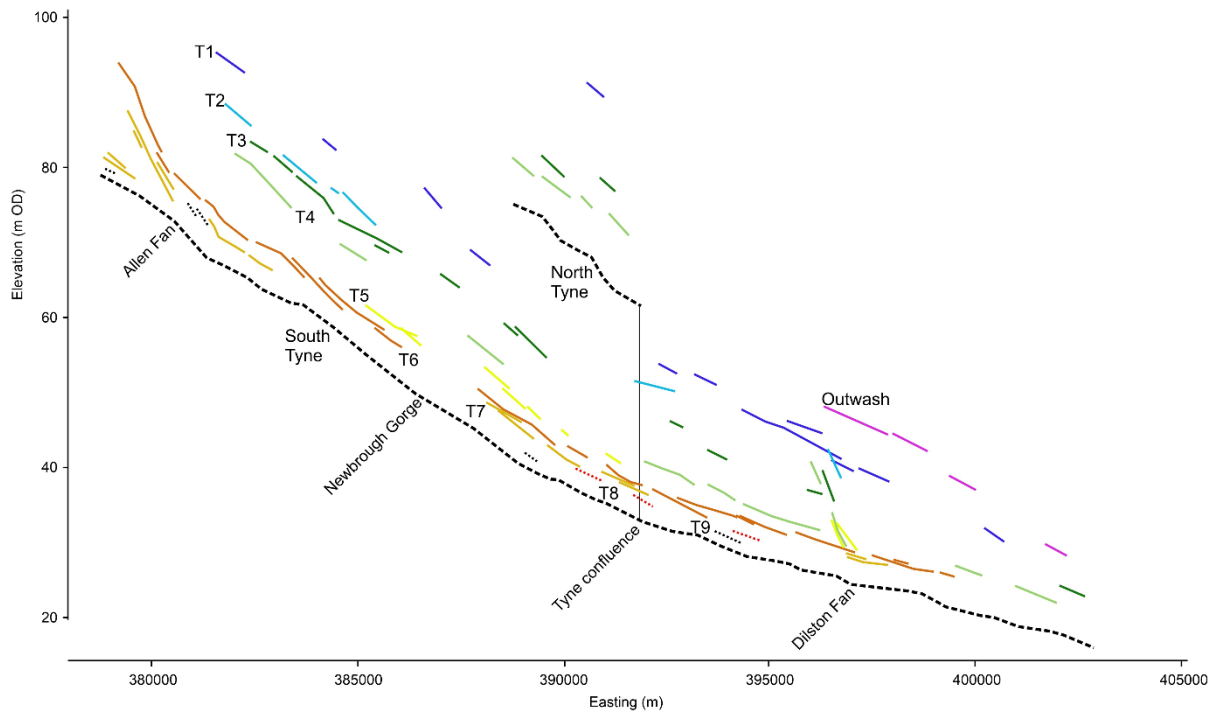


1049
 1050 Figure 1. Extent of the Tyne catchment, with key rivers and places named. Overlain on a shaded
 1051 relief SRTM DEM (Pope, 2017). The key locations in the mid-Tyne valley have been divided into
 1052 three zones (I, II and III) and are demarcated by the black rectangles.

1053

1054

1055 Figure 2. Geomorphic map of the mid-Tyne valley, showing river terraces, palaeochannels
 1056 (demarcated by double hashed lines) and alluvial fans, overlain on 1 m resolution LiDAR data and
 1057 displayed as hillshade layers (© Environment Agency copyright (2023). All rights reserved). Key
 1058 sites and localities are shown; (A) zone I, (B) zone II, and (C) zone III.



1059

1060

1061

1062

1063

1064

1065

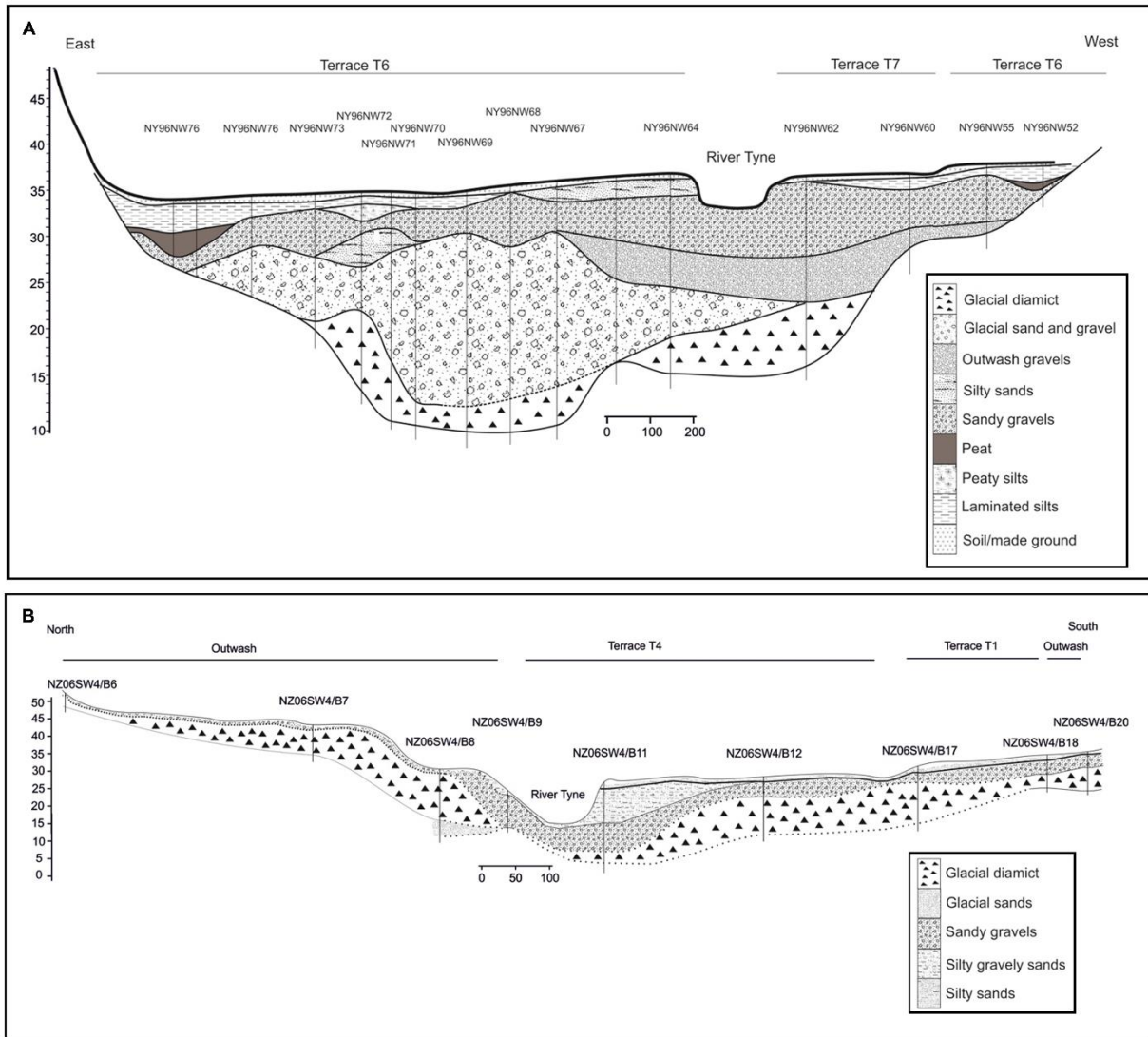
1066

Figure 3. LiDAR (© Environment Agency copyright (2023). All rights reserved) derived height range diagram for the Rivers South Tyne, North Tyne and Tyne in metres above UK Ordnance Datum (OD). Contemporary river long profiles are indicated by the dashed black lines. Differentiated river terraces are labelled T1 to T9 respectively and colour coded as follows: T1 dark blue; T2 light blue; T3 dark green; T4 light green; T5 yellow; T6 orange; T7 dark orange; T8 dashed pink; T9 dotted black lines respectively. Outwash represents the glacial terrace sequences (pink line).

1067

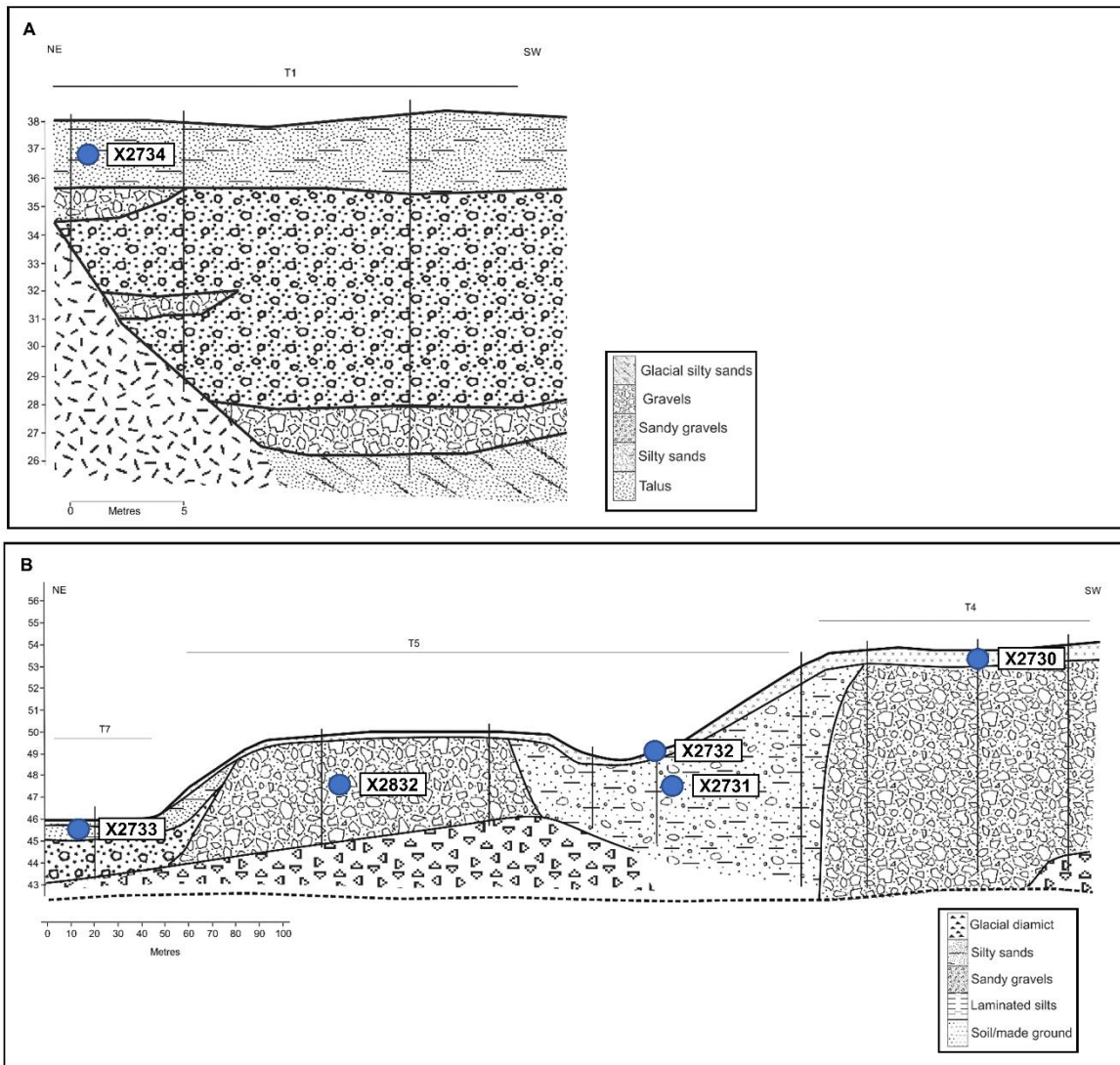
1068

1069 Figure 4. Location of (A) the A69 (road) and (B) the A68 (road) borehole transects, overlain on an
1070 Ordnance Survey 1: 25 000 Scale Colour Raster (© Crown copyright and database rights 2023
1071 Ordnance Survey). Showing mapped river terraces, palaeochannels and alluvial fans. AF, alluvial
1072 fan, T1-8, differentiated river terraces, refer to legend in figure 2.



1073

1074 Figure 5. Detailed stratigraphic and lithofacies assemblages derived from borehole data within
 1075 zones II and III. (A) the A69 (road) transect, and (B) the A68 (road) transect. Valley-floor transect
 1076 locations are shown in Fig. 4. Based upon GeoIndex (onshore) Borehole records, with the
 1077 permission of the British Geological Survey. Individual borehole records demarcated by codes
 1078 beginning with NY and NZ, with locations indicated by vertical black lines.



1079

1080 Figure 6. Farnley Haugh. (A) T1 alluvium exposed in the cut-bank on the true right-hand side of
 1081 the valley. (B) Detailed stratigraphic and lithofacies assemblage based upon interpolation of field-
 1082 gathered vertical profile logs (locations indicated by vertical black lines). The 'X' indicates the
 1083 sampling location for optically stimulated luminescence dating; lab code X2734. Estimated ages
 1084 and age ranges are compiled in Table 1.

1085

1086

1087 Figure 7. Fourstones. (A) T5 and T7 alluvium exposed on the true right-hand side of the valley.

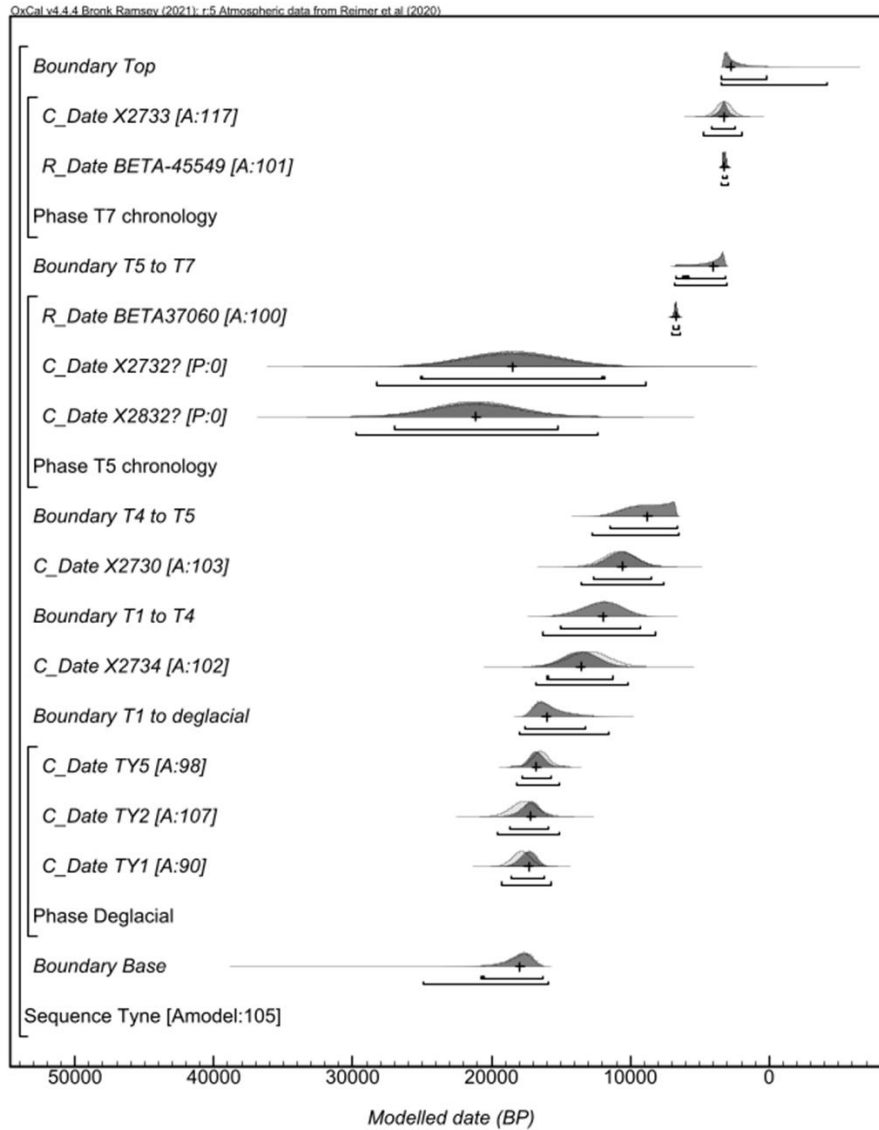
1088 (B) Detailed stratigraphic and lithofacies assemblages based upon interpolation of field-

1089 gathered vertical profile logs (locations indicated by vertical black lines). The 'X' indicates the

1090 sampling locations for Optically Stimulated Luminescence dating; lab. codes X2733 (T7), X2832,

1091 X2732, X2731 (T5), and X2730 (T4). Estimated ages and age ranges are compiled in Table 1.

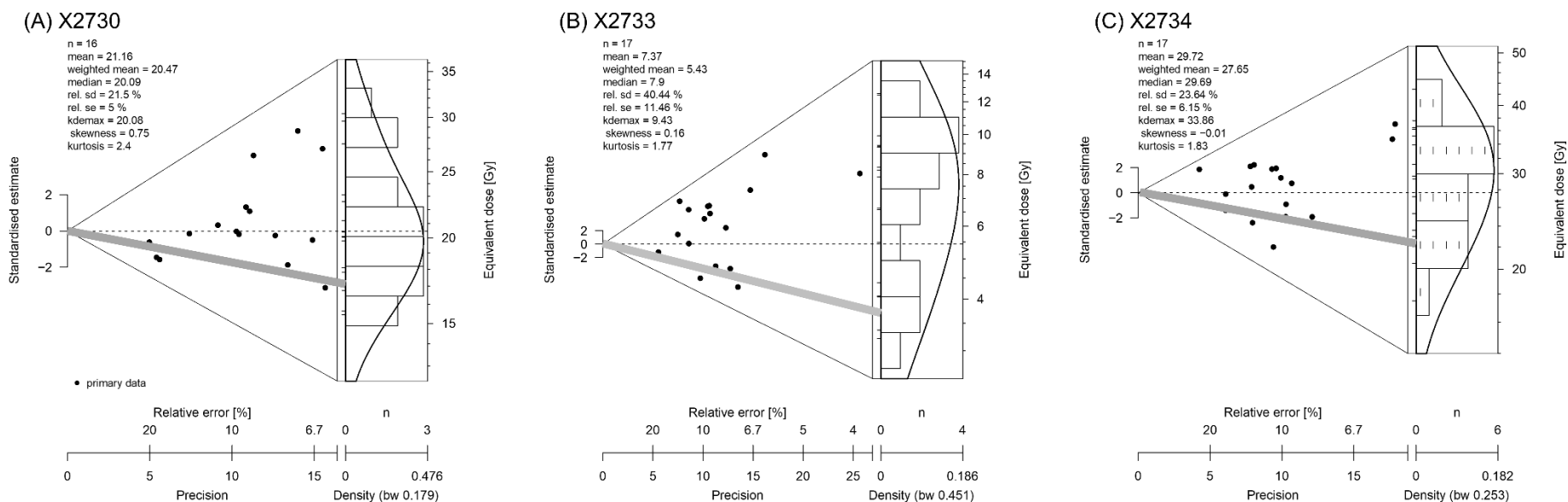
1092



1094

1095 Figure 8. Bayesian model of the dating of the Tyne terrace sequence, based on the new optically
 1096 stimulated luminescence (OSL) ages obtained by this study, alongside a published ¹⁴C age
 1097 (BETA-37060; Passmore and Macklin, 1994) and published cosmogenic ages (from boulder for
 1098 deglaciation of the Tyne Gap Ice Stream (TGIS; Livingstone et al., 2015). The model structure
 1099 shown used OxCal brackets (left) and key words define the relative order of events (Bronk
 1100 Ramsey, 2009). Modelled age in ka BP on the x-axis. Each distribution (light grey) represents the
 1101 relative probability of each age estimate with posterior density estimate (solid) generated by the
 1102 modelling. Outliers are indicated by '?' and their probability (P) of being an outlier denoted by low
 1103 values <5 (95% confidence); X2730 not shown as the date is beyond the modelled scale. Model

1104 agreement indices (A) for each age shows their fit to model, with >60% the advocated threshold
1105 by Bronk Ramsey (2009).



1106

1107

1108 Figure 9. Abanico plots of the individual aliquot equivalent does (D_e) values determined for optically stimulated luminescence dating. Plots shown are
 1109 for samples taken at (A) Fourstones X2730 (T4) and (B) Fourstones X2733 (T7), and at (C) Farnley Haugh X2734 (T1). The plots comprise two parts
 1110 (i) a bivariate plot, showing standardised estimates of D_e values in relation to precision (x-axis), and (ii) a univariate plot, showing the age frequency
 1111 distribution of D_e values but this does not give any indication of precision. Both plots are linked by the z-axis of the D_e values. Data points (or primary
 1112 data) are indicated by the black dots. Age estimates for the samples shown were determined using the MAM D_e ; the black line across the plots
 1113 represents the MAM D_e value for that sample. The abanico plots enable assessment of the data precision and the characteristics of the age
 1114 distribution; samples with a greater range of D_e values on the x-axis have a larger scatter in the D_e distribution. Samples that are well bleached before
 1115 burial typically have more symmetrical D_e distributions.

1116 **Table 1.** Summary of new optically stimulated luminescence (OSL) estimated ages and associated information for five samples from
 1117 Fourstones (south Tyne) and one sample from Farnley Haugh (Tyne). The table includes the total number of aliquots measured with OSL that
 1118 passed the acceptance criteria and the overdispersion of the resulting dose distribution. Measurements were made on dried, homogenized and
 1119 powdered material by ICP-MS/AES with an assigned systematic uncertainty of $\pm 5\%$. Dry beta dose rates calculated from these activities were
 1120 adjusted for the field water content and dose rate and age calculations were obtained using DRAC ver1.2 (Durcan et al. 2015).

Location	Lab code	Depth (m)	W* (%)	Cosmic dose rate (Gy/ka)	Total dose rate (Gy/ka)	Aliquots accepted (measured)	Equivalent dose ⁺ (Gy)	Over-dispersion (%)	Age estimate ⁺⁺ (ka)
Fourstones	X2730	0.70	18	0.19 \pm 0.02	1.91 \pm 0.02	16 (18)	21.09 \pm 2.04	17.10	10.77 \pm 1.13
	X2731	5.50	18	0.11 \pm 0.01	0.90 \pm 0.06	14 (18)	57.67 \pm 10.89	35.70	61.98 \pm 11.98
	X2732	2.00	18	0.16 \pm 0.01	0.98 \pm 0.06	17 (18)	18.54 \pm 3.29	53.60	18.51 \pm 3.36
	X2733	0.90	18	0.19 \pm 0.02	1.22 \pm 0.08	17 (17)	4.03 \pm 0.66	41.70	3.24 \pm 0.54
	X2832	3.00	24	0.14 \pm 0.01	2.56 \pm 0.17	11 (12)	57.18 \pm 7.78	22.80	21.13 \pm 2.99
Farnley Haugh	X2734	2.00	12	0.16 \pm 0.01	2.45 \pm 0.01	17 (17)	28.80 \pm 2.96	20.40	12.96 \pm 1.44

1121
1122

1123 * The recorded moisture contents (values in brackets) are not considered to be representative of the mean water content of the sediment
 1124 during the burial period as a result of recent (<20years) bank migration and/or quarrying activity. The dose rate calculations are based on
 1125 more realistic saturation estimates with an associated error of $\pm 5\%$.

1126 + OSL measurements were made with an automated TL/DA-15 Risø luminescence reader (Bøtter-Jensen, 1997; Bøtter-Jensen et al., 2000)
 1127 and conducted on 180–250 μ m or 90-125 μ m diameter quartz grains mounted as multigrain aliquots (n=12-17). The equivalent dose (De) was
 1128 obtained using a single-aliquot regeneration (SAR) measurement protocol (Murray and Wintle, 2000; Wintle and Murray, 2006) and was based
 1129 on a minimum age model after Galbraith et al. (1999).

1130

1131 ++ The age datum refers to AD 2007 when the samples were measured and the luminescence dates. The total uncertainty (1σ), calculated
1132 as the quadratic sum of the random and systematic errors, includes all measurement uncertainties as well as a relative error of 2% to
1133 account for possible bias in the calibration of the laboratory beta source.